STUDY OF DISTURBANCE OBSERVER BASED CONTROLLERS FOR MOTION CONTROL SYSTEM

A Thesis Submitted in Partial Fulfilment of the Requirements for the

Degree of Master of Electrical Engineering

By

SANDIPAN DEB

Examination Roll No.: **M4ELE19013**

Registration No. : **140656 of 2017-18**

Under the guidance of

Prof. SMITA SADHU

Electrical Engineering Department

Faculty of Engineering and Technology

JADAVPUR UNIVERSITY

KOLKATA- 700032, W.B. INDIA

May, 2019

JADAVPUR UNIVERSITY

FACULTY OF ENGINEERING AND TECHNOLOGY

ELECTRICAL ENGINEERING DEPARTMENT

KOLKATA- 700032, INDIA

CERTIFICATE OF RECOMMENDATION

I hereby recommended that the thesis titled "**STUDY OF DISTURBANCE OBSERVER BASED CONTROLLERS FOR MOTION CONTROL SYSTEM** ", submitted by **SANDIPAN DEB** (Registration No. 140656 of 2017-18), in partial fulfilment of the requirement for the degree of "Master of Electrical Engineering" of Jadavpur University has been carried out by him under my guidance and supervision.

SUPERVISOR

____

Prof. Smita Sadhu

Professor

Electrical Engineering Department,

Jadavpur University

COUNTERSIGNED

____

Prof. Kesab Bhattacharyya

Head, Dept. of Electrical Engineering,

Faculty of Engineering and Technology,

Jadavpur University

____

Prof. Chiranjib Bhattacharjee

Dean,

Faculty of Engineering and Technology,

Jadavpur University

JADAVPUR UNIVERSITY

KOLKATA- 700032, INDIA

<u>FACULTY OF ENGINEERING AND TECHNOLOGY</u>

<u>ELECTRICAL ENGINEERING DEPARTMENT</u>

CERTIFICATE OF APPROVAL*

The foregoing thesis is hereby approved as a credible study of Master of Electrical Engineering and presented in a manner satisfactory to warrant its acceptance as a prerequisite to the degree for which it has been submitted. It is understood that by this approval the undersigned does not necessarily endorse or approve any statement made, opinion expressed or conclusion therein but approve this thesis only for the purpose for which it is submitted.

Final Examination for Evaluation of the Thesis

1. ______________________________

2. ______________________________

(Signature of Examiners)

*Only in case the thesis is approved

DECLARATION OF ORIGINALITY AND COMPLIANCE OF ACADEMIC ETHICS

I hereby declare that the thesis entitled "**Study of Disturbance Observer Based Motion Control System**" contains literature survey and original research work as part of the course of Master of Engineering studies. All the informations in this document have been obtained and presented in accordance with academic rules and ethical conduct.

I also declare that, as required by these rules and conduct, I have fully cited and referenced all material and results that are not original to this work.

Name	:	SANDIPAN DEB
Exam Roll no.	:	M4ELE19013
Registration no.	:	140656 of 2017-18
Thesis Name	:	STUDY OF DISTURBANCE OBSERVER BASED CONTROLLERS FOR MOTION CONTROL SYSTEM
Signature with date	:	

ACKNOWLEDGEMENT

With a great pleasure, I express my deep sense of gratitude to my supervisor, **Prof. Smita Sadhu,** Department of Electrical Engineering of Jadavpur University for giving me the invaluable opportunity to work in this exciting field. I am obliged and grateful to her for guidance, suggestions and encouragement throughout the project. I will always remain thankful to her for her patience with me. As a beginner in this field, I learn how to do research work from her.

I would also wish to express my sincere gratitude to **Professor Tapan Kumar Ghoshal, Professor Sayantan Chakraborty, Professor Ranjit Kumar Barai,** Department of Electrical Engineering, Jadavpur University, for their encouragement, advice and motivation during the coursework.

I am also thankful to **Dr. Kesab Bhattacharyya**, Head, Department of Electrical Engineering, Jadavpur University, for providing the necessary facilities for carrying out this research work.

I am taking the opportunity to express my humble indebtedness to **Mr. Nialanjan Patra** research scholar, for his invaluable inputs during this work.

I would like to thank my dear friend **Mr. Banibrata Ghosh, Ms. Medha Nag**, PG scholar, E.E. Department, from whom I received immense support, inexplicable encouragements and assistance. I would like to convey my soulful thankfulness to the rest of the PG scholars of E.E. Department for their moral support during this course work. I am extremely grateful to my parents for their constant support and motivation, without that I would not have come to this stage. This thesis, a fruit of the combined efforts of my family members, is dedicated to them as a token of love and gratitude.

Above all, it is the wish of the almighty that I have been able to complete this work.

Thank you,

Sandipan Deb

DEDICATED TO MY PARENTS

Abstract

Disturbance exists in almost all kind of systems, which does mean not only external disturbances but also the system parameter uncertainties. It brings adverse effects on the desired performance of the system. Therefore, disturbance estimation and rejection are equally necessary for desired response of a system. Researchers found that Disturbance Observer provides an effective disturbance estimation technique for a wide range of systems.

This dissertation is about verification and modification of DOB based Motion Control System, followed by disturbance estimation and suppression. At first, DOB design method has been studied. Then system response is analysed without any disturbance observer. Next, external disturbance along with parameter uncertainties are estimated by Disturbance Observer with and without the outer loop controller. Then, PID and PD both controllers are used separately to achieve performance goals. Finally, performance comparison has been made between the existing PD controller and DOB, and proposed PID controller and DOB using MATLAB.

CONTENTS

LIST OF FIGURES

NOMENCLATURE

DOB	Disturbance Observer
RTOB	Reaction Torque Observer
LPF	Low Pass Filter
BW	Bandwidth
DOF	Degree Of Freedom
PADC	Passive Anti-disturbance Control
AADC	Active Anti-disturbance Control
DOBC	Disturbance Observer Based Control
PID	Proportional Integral Derivative
PD	Proportional Derivative
MCS	Motion Control System

CHAPTER 1

INTRODUCTION

1.1 Background:

Motion control is one of the most important technology in mechatronics. It encompasses every technology related to the movement of objects. Now-a-days, the focus of motion control deals with special control technology of motion systems with electric actuators such as dc or ac servo motors. Technologies like robot manipulators are driven by electrical servo motors, as a result robot manipulators are also included in the area of motion control field. With the advancement of power electronics and computer technology it is easier to improve the performance of motion control. Due to availability of vector control, ac servo motors can be designed with same characteristics as dc motors. To summarize the development of motion control technology, the following figure [25] is represented below.

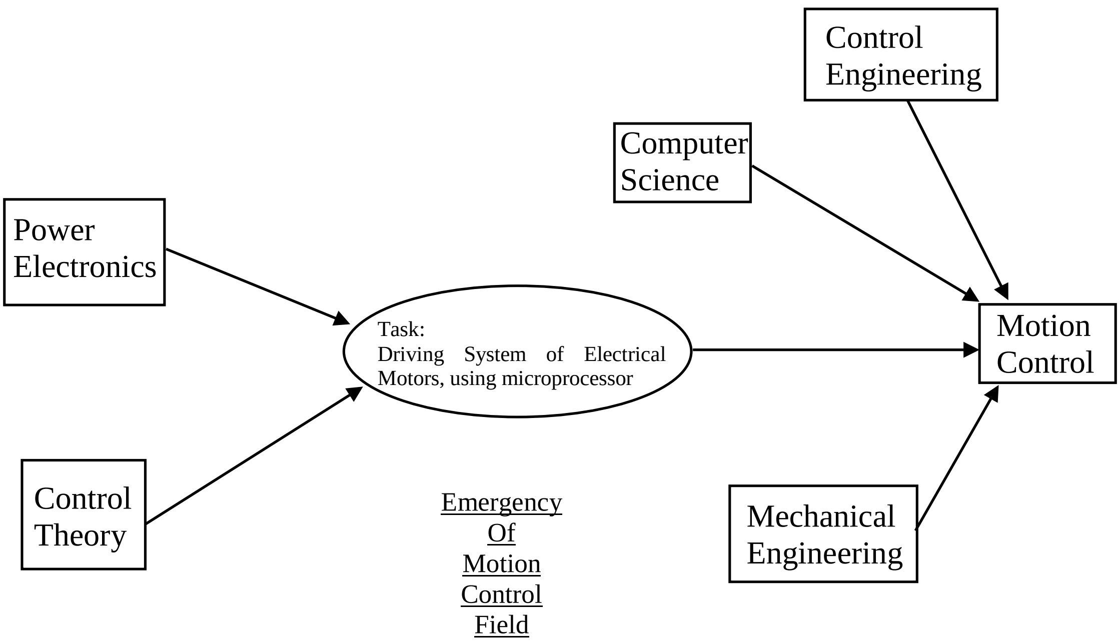

Fig.1.1- Development of Motion Control field [25]

Theory of Motion Control:

Motion controllers and reference generators build a complete motion control. The dynamics of a mechanical system governed by lagrange's equations [25] can be described by some set of differential equations which gives the constraints of motion. Those equations are based on dynamic equilibrium of force. As per the motion reference, motion controller generates some set of inputs to the actuator. A motion reference is now produced followed by some complex algorithms in reference generator which has a composite structure. Inputs to this reference generator can be taken from output signal of a sensor or commands from human operator.

The output of motion control is either position or force. Trajectory tracking is an example of position control and simple mass spring system can be considered as an example of force control considering the forces of contacts. Stiffness (κ) is an important indices which covers various motion.

Let, x is position of an object and F be the imposed force on it which is a function of x. According to the dynamic equation [3]-

$$F = f(x, \dot{x}, \ddot{x})$$

By taking partial differentiation, we can get stiffness :

$$\kappa = \frac{\partial F}{\partial x}$$

For ideal position control, κ value should be infinite as there should be deviation of force with any deviation of position. And for ideal force control κ value should be zero as there should be deviation of position with any deviation of force. In compliance control there is a relation between position and force control resulting the κ value to be finite.

Now for the motion systems, the stability is generally affected by different external disturbances- like uncertain torque disturbances, load torque variation. Moreover, the control performances are also affected by internal model parameter perturbations caused by the changes of operation conditions and external working environments. So the solution to the disturbance rejection is a necessary task since the starting of control system and its applications. Researchers found strong algorithms for disturbance attenuation giving higher control precision and production efficiency of practical engineering systems. Some methods of disturbance rejection are described below.

A. **Adaptive control**: This method helps rejecting undesired effects due to structure parameter uncertainties. At first, system parameters are estimated online, then they are tuned in order to get desired performance. This method does not work when those system parameters are hard to estimate online.

B. **Robust Control**: This is a over-conservative method as it considers worst case parameter uncertainties. Robustness can be achieved by sacrificing the transient response by this method.

C. **Sliding Mode Control**: It can attenuate external disturbance and parameter variation. But the main problem of this method is high frequency chattering. Though chattering can be taken care of by saturation method but active disturbance rejection is compromised.

D. **Internal Model Control**: This method handles the effects of external disturbance. Its simple concept makes it widely applicable in control domain and application part. It is used for linear system only cutting down its wide range of application in non-linear system.

Those above mentioned methods suppress disturbances by feedback control instead of feedforward compensation control. So, when strong disturbances are present these methods work in slow way via feedback regulation. That's why they are called passive anti-disturbance control (PADC).

PADC method can suppress disturbance but to get faster disturbance rejection active anti-disturbance control (AADC) method was invented. It directly deals with the disturbance by feedforward compensation estimating the disturbance.

Traditional feedback control is the first AADC method. Here, a sensor is used to measure the disturbance. Then disturbance channel model is built. At last, a feedforwad controller is designed. The whole system counteracts the disturbances. But, in most of the practical systems disturbances are difficult to measure also parameter uncertainties make the system performance worse.

Taking the advantage of FC and the mentioned disadvantage into account, effective disturbance estimation techniques needed to be invented. Disturbance Observer (DOB) is the most effective and popular approach to reject disturbances as robustness can be achieve in a desired bandwidth. It was first invented by K. Ohnishi in 1983. It is now widely used in both control theory and control application fields. The working principle of DOB along with block diagram has been described in details in chapter 3 [26].

1.2 Motivation:

In conventional analysis and design methods of control systems it is assumed that plant dynamics is known whereas the assumption is not true in practical cases. So, if a controller is designed on the basis of identified plant model then the stability and performance may deteriorate. Apart from these parameter uncertainties external disturbances is also present, and Motion Control system is not an exceptional from control point of view. So, to improve the stability and performance of MCS plant uncertainties and external disturbances should be taken into consideration. To achieve this, several 2-DOF controllers are widely used in industries. Among them DOB is one of the most popular methods as the robustness can be achieved in a desired BW. Although DOB is widely used in several applications, the trade-off between robustness and stability in design of a DOB was not proposed since 2015. **E. Sariyildiz** and **K. Ohnishi** proposed a new design criteria to adjust the trade-off, in addition a new stability analysis method for force control was proposed by them [24]. But in this thesis work, main focus is on position control system. The new design criteria [24] has been verified in this thesis work. Also, with a motive to improve stability and performance PID controller has been used in outer-loop. PID controller and DOB based position control system has been analysed in detail. Finally, a comparison of performance between the existing PD controller & DOB and Proposed PID controller & DOB based position control system has been done in this thesis work.

1.3 Thesis Objective:

The main objective of the thesis are stated as follows:

- To study the DOB based position control system with existing PD Controller, verifying the trade-off between robustness and stability while designing the DOB [24].
- To estimate the disturbance and to check disturbance rejection on existing DOB based position control system.
- To analyse the proposed PID controller based position control system in terms of stability, robustness. Then to estimate the disturbance and to check disturbance rejection on the same.
- To compare the existing PD controller based DOB and proposed PID controller based DOB through disturbance estimation error, tracking error.

1.3 Salient Contributions:

This section states the contribution of the present work in the background of the earlier work.

- Verification of the design methods for robustness and stability analysis for existing DOB based position control system [24].
- Estimation of disturbance using a set of different input waveforms as disturbance on existing DOB based position control system using SIMULINK model.
- Trajectory checking on existing DOB based position control system.
- Modelling PID controller and DOB based position control system. Hence, analysing it followed by disturbance estimation, trajectory tracking.
- To compare the disturbance estimation error (DEE) and tracking error (TE) between existing PD controller based DOB and proposed PID controller based DOB.

1.4 Organisation Of the thesis:

The entire thesis work has been described in seven chapters as follows-

In **chapter 1**, a brief overview of motion control system is described. Then, brief discussion including advantages and disadvantages of anti-disturbance control methods are described. Finally, evolution of DOB is discussed

In **chapter 2**, literature survey has been done in details on DOB and its implementation on motion control system.

In **chapter 3**, design of DOB has been described with examples.

In **chapter 4**, motion control system has been depicted with block diagram. Then implementation of DOB on motion control has been discussed followed by disturbance estimation, stability and robustness analysis.

In **chapter 5**, PID controller based DOB has been proposed. Then robustness and stability analysis have been done analytically. Disturbance estimation and position tracking is done using SIMULINK model.

In **chapter 6**, comparative study on DEE and TE have been done on the above mentioned methodologies.

In **chapter 7**, the dissertation ends by this section giving conclusions and future scope of research in this domain.

Chapter 2

LITERATURE REVIEW

2.1 Introduction:

In this survey a brief summary of DOB based motion control system has been described.

2.2 Literature survey:

Robust servo-system design method based on 2-DOF controller was proposed by **T. Umeno** in 1993. The servo-system is derived from simple parametrization. The close loop characteristics and input response can be controlled separately. Then the 2-DOF controller is used in advanced motion control [1].

T. Murakami, F. Yu, and K. Ohnishi [2] presented a torque sensorless control in multi-degree of freedom manipulator. In one joint the DOB is used to calculate the disturbances and another one is used to calculate reaction force once the disturbance is estimated. Then it is expanded to workspace force control in multi-degree of freedom manipulator.

After the emergence of motion control, the connection between robustness and variable stiffness needed to be done. **K. Ohnishi, M. Shibata, and T. Murakami** [3] showed control of acceleration realizes specified motion while keeping robustness high. In this paper, Motion control of flexible structure and identification of mechanical parameters are also described.

For reading and writing hard disk drives' a 2-DOF control structure was proposed by **L. Yi** and **M. Tomizuka** [4]. The new features in this paper are a new method for generating reference signal for track seeking, and another is adaptive robust control method. Control with ARC provides better performances than conventional servo system or 2-DOF structure with DOB. Later decentralized adaptive robust control for trajectory tracking was proposed by **Z.Yang, Y. Fukushima** [5]**.** After that, 4-channel bilateral control design for haptic communication under time delay was proposed by **A.Suzuki** and **K.Ohnishi** [6]. But, most of DOB based plants are SISO type. For application to MIMO plants a control structure that reduces it to SISO was also proposed [7]. There are other applications of DOB are there like biped walking robots [8], permanent magnet linear motors etc. [9].

A new controller architecture was proposed by **K.Zhou** and **Z. Ren** [10] to control separately the robustness and performance that can overcome the problem faced in conventional feedback framework. In absence of disturbances only performance controller will work and in presence of disturbance robustification controller will also be active.

In 2005, "law of action and reaction" by multilateral control was introduced by **S.Katsura, Y.Matsumoto, K. Ohnishi.** [11]The design of bilateral control based on DOB has been done here, the design is treated as position and force control in a single joint. Then it is generalized as multilateral control based on modal decomposition.

Although, DOB based controllers are used in industries widely but there was no necessary and sufficient condition for robust stability until 2009. **H.Shim, N.H. Jo** [12] proposed the same when Q-filter has sufficiently small time constant. If the nominal system is minimum phase and outer loop controller stabilizes the nominal system then the proposed theory would give robustness under large parameter uncertainties. To get more ideas about outer loop controller performance study, application of variable structure systems in motion control has been studied [13].

Now, the bandwidth limitation due to noise and robustness constraints was still there because of conservatism. In 2013 a new robust stability analysis method was proposed by **E.Sariyildiz, K.Ohnishi.** [14] It has been showed that a lower bound exists for bandwidth of DOB to obtain robust stability, if the BW increases then robustness also increases. Then for non-minimum phase case the upper and lower bound of BW has been discussed by the same authors [15]. The noise suppressing techniques to improve bandwidth constraints has been discussed in the following papers [16]-[18].

H. Kobayashi, S. Katsura, K.Ohnishi proposed parameter variation limitation and though only inertia variation had been taken into consideration, then stability of position and force control had been analysed [19].

A RTOB estimates the environmental impedance which is an application of DOB. Like DOB, the force control BW has been studied in the following literature [2], [20]-[22]. Advantages over a force sensor has also been discussed in the aforesaid literature. The recent studies on adaptive reaction force observer has also been studied [23]. Here the design parameters like inertia, BW of DOB and RTOB, force control gain is adjusted by adaptive algorithm providing good stability and robustness considering the design constraints of DOB.

Chapter 3

BRIEF OVERVIEW OF DISTURBANCE OBSERVERS

3.1 Introduction:

In general, there are two types of disturbance rejection methods, one is PADC and another one AADC. DOB is in AADC category. Here only DOB has been described in details as it is more effective to deal with disturbance and giving robustness than high gain control and integral control methods.

3.2 Basic framework of DOBC:

The basic framework of DOBC is shown below

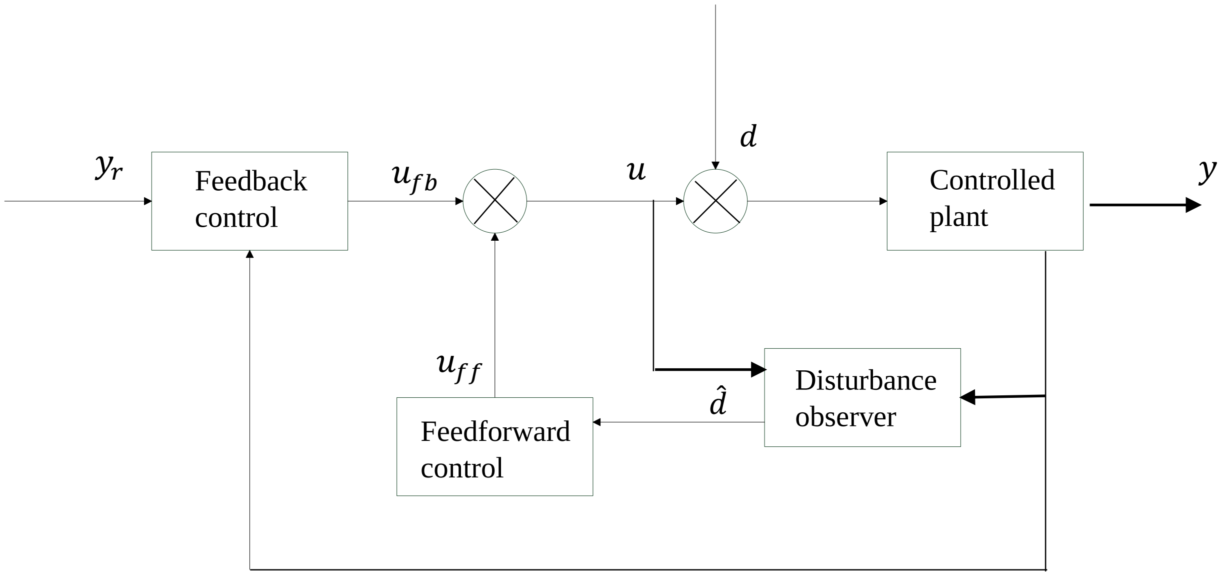

Fig. 3.1- A basic framework of DOBC [26]

It is seen from the figure that the whole system consists of two parts, one is feedback control part another is feedforward control part. First one is used to track and stabilize the nominal control plant. This part doesn't consider plant uncertainties and external disturbances. The DOB estimates the disturbances and uncertainties and then it is compensated by feedforward control. The disturbance rejection and tracking control can be done separately which is a major advantage of DOBC method. The comparison with the PADC method is shown below:

- **Faster response:** Feedforward control directly counteracts with disturbances giving faster response of the system in case of DOBC. But PADC attenuates disturbances by passive feedback regulation.

- **Patch feature:** The term ‘patch’ refers to the feedforward control part to the existing feedback control. Once the feedback control part is done, DOB is introduced to improve plant responses under the effect of disturbances and uncertainties.
- **Less conservative:** Unlike robust control, DOBC is not designed taking worst case scenario. So, it doesn’t compromise with the nominal plant dynamics performance. In absence of any parameter uncertainties or disturbances DOBC recovers the baseline controller is recovered resulting better nominal plant performance.

3.3 Disturbance Observer design:

In this section, disturbance observer design has been discussed [26]. Here, the disturbance estimation technique is limited to only frequency domain formulation. At first the minimum phase case is described as follows:

3.3.1 DOB design for minimum phase systems:

Let us consider a SISO minimum phase system depicted as follows-

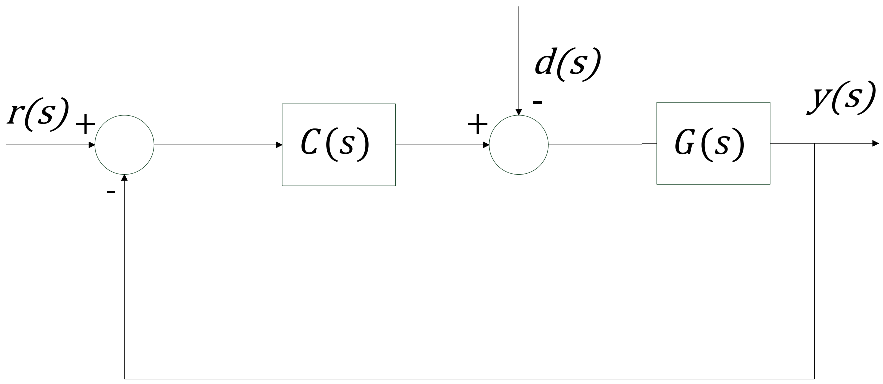

Fig. 3.2- Block diagram of a basic feedback control system

So, the output of the system can be written as-

$$y(s) = T_{ry}(s)r(s) + T_{dy}(s)d(s) \quad (3.1)$$

Where r(s) is the reference input, y(s) is output, C(s) is controller transfer function, G(s) is plant transfer function, $T_{ry}(s)$ is transfer function from reference input to output, $T_{dy}(s)$ is transfer function from disturbance input to output.

Now, based on the equation (3.1), DOB in frequency domain can be drawn as-

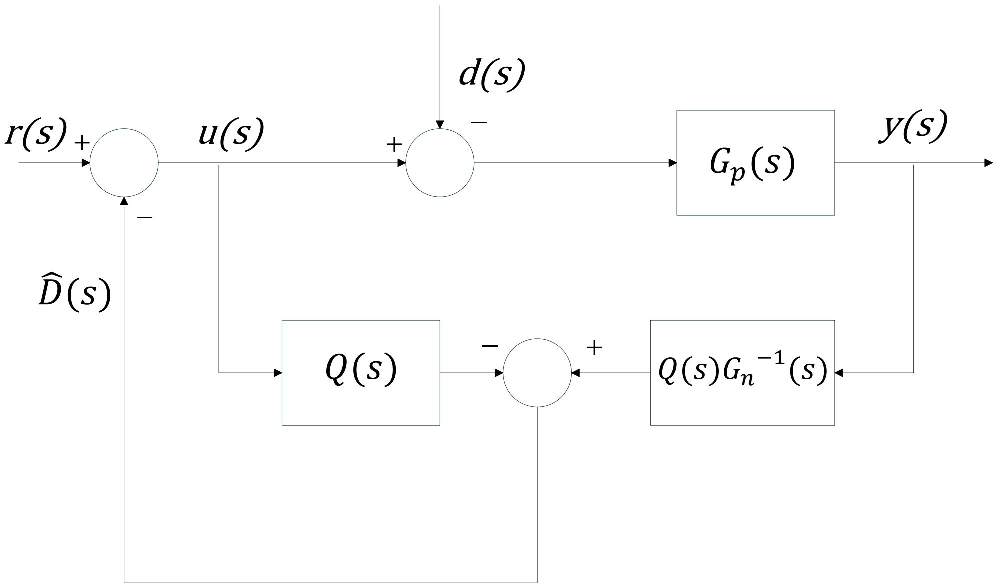

Fig. 3.3a- Block diagram of a frequency domain DOB for minimum phase linear system, an original form [26]

$Q(s)$ is the transfer function for low pass filter. $G_n(s)$ is nominal plant transfer function and $G_p(s)$ is plant transfer function with parameter uncertainties. Now, for the disturbance estimation considering external and internal both, lumped disturbance has been taken which is shown as the following figure-

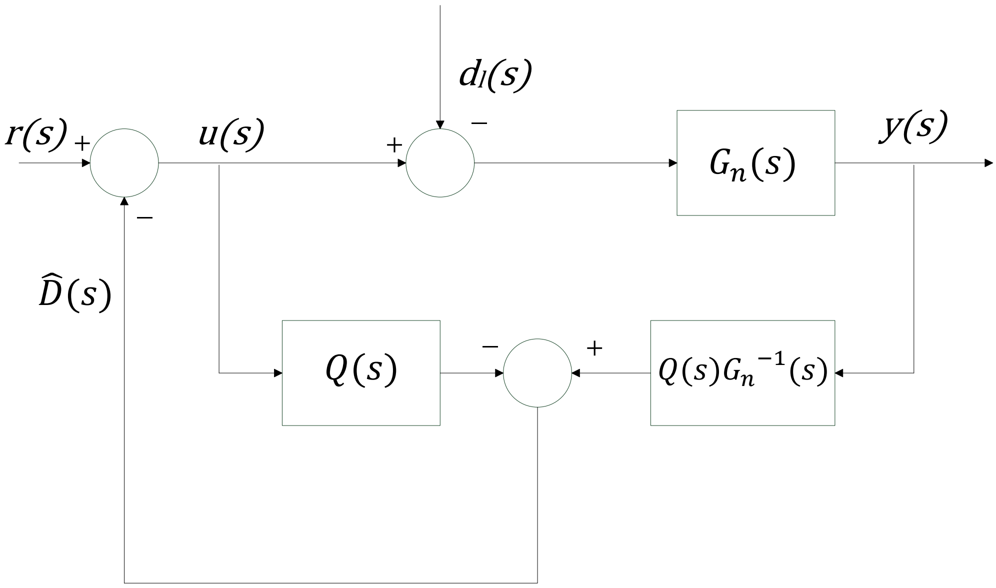

Fig. 3.3b- Block diagram of a frequency domain DOB for minimum phase linear system, an equivalent form [26]

$$\hat{d}(s) = Q(s)G_n^{-1}(s)y(s) - Q(s)u(s) = Q(s)G_n^{-1}(s)[u(s)+d_l(s)]G_n(s) - Q(s)u(s) \quad (3.2)$$

as y(s) can be written as $\{u(s)+d_l(s)\}G_n(s)$

So,

$$\hat{d}(s) = Q(s)d_l(s) \quad (3.3)$$

Again,

$$e_d(s) = \hat{d}(s) - d_l(s) = [Q(s) - 1]d_l(s) \quad (3.4)$$

If the filter Q(s) is taken as low pass filter then e_d(s) will tend to zero as time goes to infinity.

This means, $\lim_{s\to 0} Q(s) = 1$.

Again, output is derived in terms of input r(s) and disturbance d(s) as-

When, d(s)=0, we find $T_{ry}(s)$. Reducing the block diagram of fig. (3.3a) to

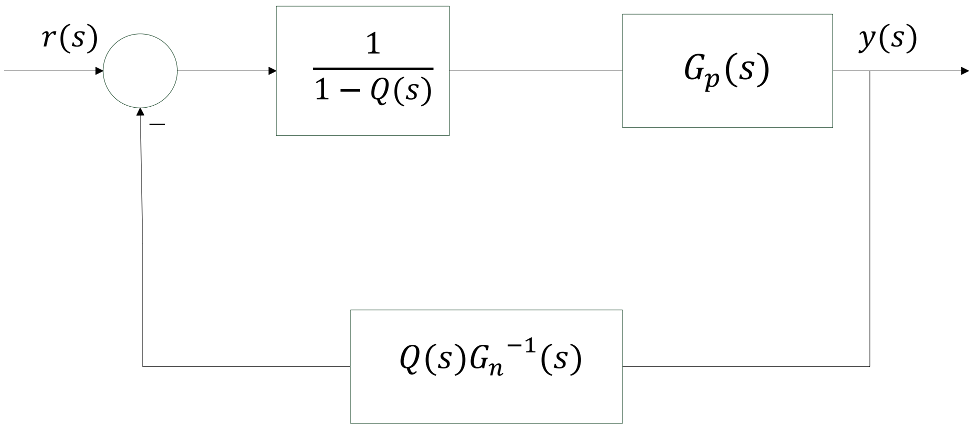

Fig. 3.4- Simplified block diagram of fig. (3.3a)

So,

$$T_{ry}(s) = \frac{G_p(s)G_n(s)}{G_n(s)+Q(s)[G_p(s)-G_n(s)]} \quad (3.5)$$

It can be seen if Q(s)=1 then, $T_{ry}(s)$ becomes-

$$\lim_{\omega\to 0} T_{ry}(j\omega) = G_n(j\omega) \quad (3.6)$$

This equation (3.6) signifies that in low frequency domain the system response is same as that of nominal plant transfer function.

Now, to find the transfer function of $T_{dy}(s)$, r(s) should be taken as 0. The reduced BD becomes-

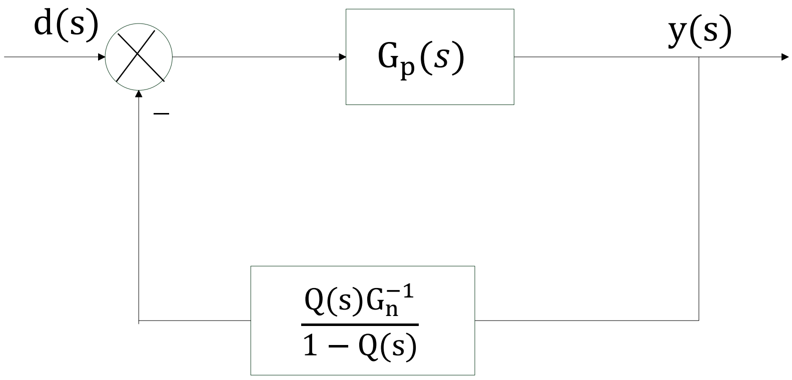

Fig. 3.5- Simplified block diagram of fig. (3.3a)

So,

$$T_{dy}(s)= \frac{G_p(s)G_n(s)[1-Q(s)]}{G_n(s)+Q(s)[G_p(s)-G_n(s)]} \quad (3.7)$$

It can be seen from (3.7) that if Q(s)=1 then

$$\lim_{\omega\to 0} T_{dy}(j\omega) = 0 \quad (3.8)$$

This equation (3.5) signifies the disturbances have been rejected in low frequency domain. It is also seen that design of Q(s) strongly determines the disturbance estimation. So, the design criteria of Q(s) can be stated as follows-

- The transfer function $Q(s)G_n^{-1}(s)$ should be realizable, i.e. it should be proper function. To ensure this criteria the relative degree of Q(s) should not be less than that of $G_n(s)$.
- As Q(s) approaches 1 in low frequency domain, estimated disturbance becomes same as lumped disturbance. Hence, it can be said the disturbances have been successfully attenuated by feedforward compensation based on disturbance observer.

Numerical example to design Q(s) for minimum phase system:

Let a nominal plant transfer function

$$G_n(s) = \frac{(s+1)}{(s+2)(s+3)}$$

It is assumed that there is no uncertainties in the system. So, the transfer function of $G_p(s)$ is same as $G_n(s)$, r(s) is taken as step input of magnitude 1 applied at t=0.

According to the design criteria for Q(s) mentioned above, it is taken as first order LPF to make $Q(s)G_n^{-1}$ realizable. So, Q(s) is taken as

$$Q(s) = \frac{1}{\lambda s+1}, \text{ So, } Q(s)G_n^{-1}(s) = \frac{(s+2)(s+3)}{(s+1)(\lambda s+1)}$$

Now that $Q(s)G_n^{-1}$ has become proper function it can be realized. The disturbance estimation accuracy is determined by λ value. Again from equation (3.4) it can be said that disturbance estimation depends on frequency characteristics of {1-Q(s)} implying smaller the value of λ, smaller will be the disturbance estimation error.

Here, disturbance d(t) is taken as

$$d(t) = \begin{cases} \sin(t), 0 \leq t \leq 1 \\ 1 + \sin(t), t > 1 \end{cases}$$

Responses for the system shown below-

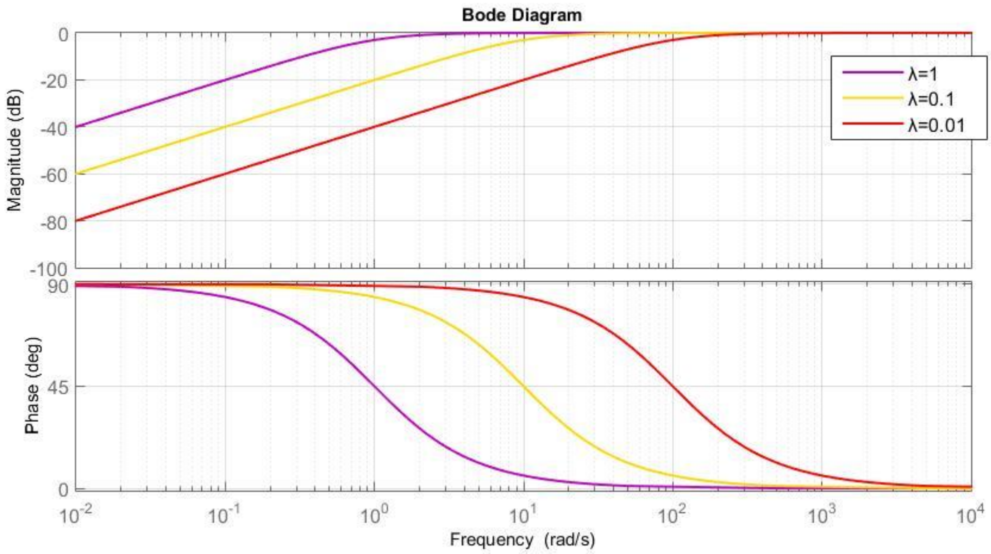

Fig. 3.6- Bode plot for different λ values

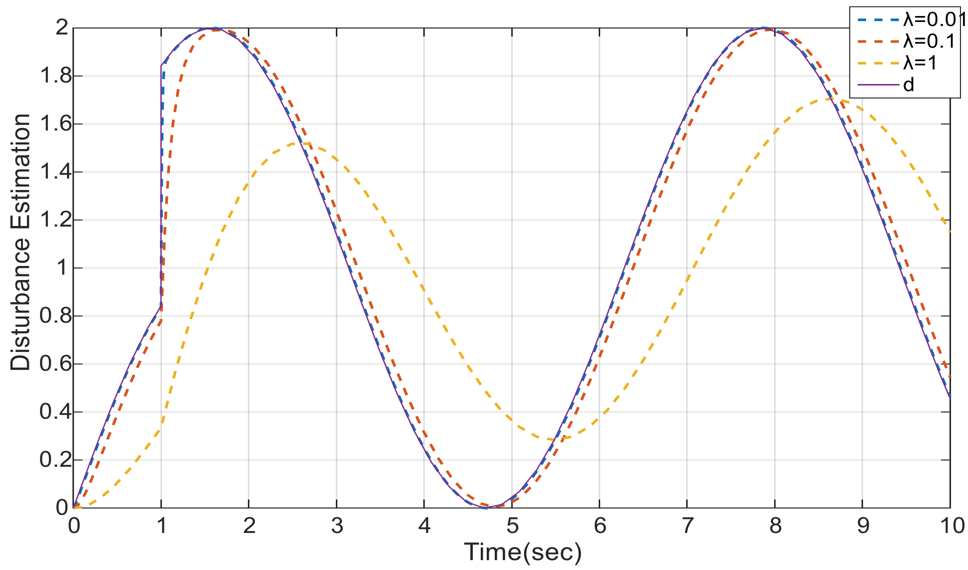

Fig. 3.7- Disturbance estimation plots for different λ values

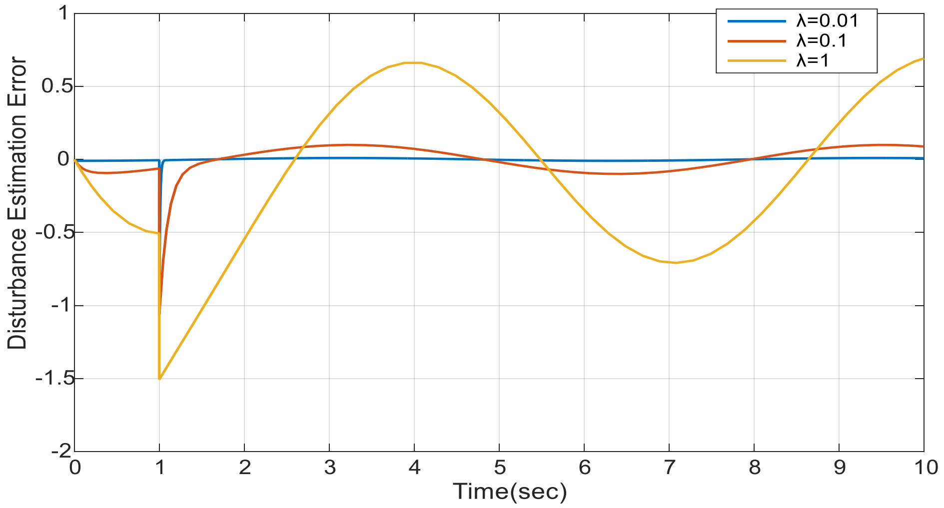

Fig. 3.8- Disturbance estimation error plots for different λ values

Observations:

It can be seen form the figures, by choosing small λ value, disturbance estimation can be done more precisely. Here, for $\lambda = 0.01$, the disturbance observer maintains the error almost zero except at t=1 sec as there is a spike in error plot.

3.3.2 Non-minimum phase case:

Let a nominal plant transfer function $\mathrm{G_n(s)}$ is taken as –

$$\mathrm{G_n(s)} = \frac{k(1-\beta s)}{(\alpha_1 s+1)(\alpha_2 s+1)}$$

α_1,α_2,β are positive real numbers. There is a RH zero in the above TF. Again the low pass filter is taken as

$$\frac{1}{\lambda s + 1}$$

Now, following the same method mentioned for minimum phase system, the transfer function $\mathrm{Q(s)G_n^{-1}}$ becomes:

$$\frac{(\alpha_1 s + 1)(\alpha_2 s + 1)}{(\lambda s + 1)k(1 - \beta s)}$$

By doing this, the RH zero of the nominal plant becomes RH pole for DOB making the observer unstable. So, this method is not applicable for non-minimum phase systems. So, if a plant has RH zeroes, then it should be factored out before doing the inverse for observer designing. There are so many methods [26], but all pass factorization is used here. It places the zero in non-invertible part and, a pole is also placed at the reflection of the RH zero. The system $G_n(s)$ is factored as-

$$G_n(s) = G_{n-}(s)G_{n+}(s)$$

Where, $G_{n-}(s) = \frac{k(1+\beta s)}{(\alpha_1 s+1)(\alpha_2 s+1)}$, $G_{n+}(s) = \frac{k(1-\beta s)}{(1+\beta s)}$

The steady-state gain is 1 for $G_{n+}(s)$. The BD for frequency domain DOB is shown as-

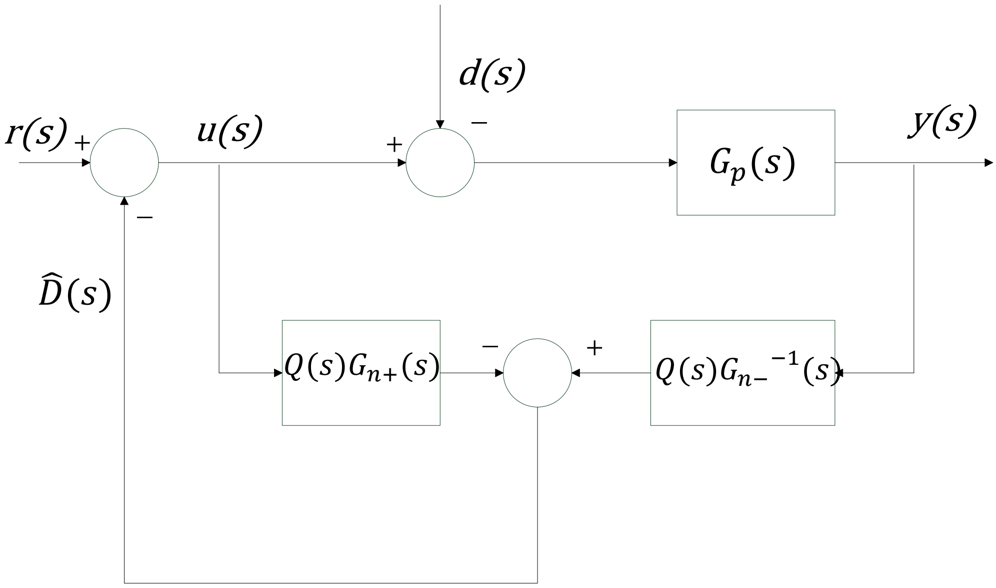

Fig. 3.9- BD of a frequency domain DOB for non-minimum phase linear system [26]

The output y(s) can be written as-

$$y(s) = T_{ry}(s)r(s) + T_{dy}(s)d(s) \tag{3.9}$$

Where, $$T_{ry}(s) = \frac{G_p(s)G_{n-}(s)}{G_{n-}(s)+Q(s)[G_p(s)-G_n(s)]} \tag{3.10}$$

And, $$T_{dy}(s) = \frac{G_p(s)G_{n-}(s)[1-G_{n+}(s)Q(s)]}{G_{n-}(s)+Q(s)[G_p(s)-G_n(s)]} \tag{3.11}$$

It can be deduced that, $\lim_{\omega\to 0} G_{n+}(j\omega) = 1$, $\lim_{\omega\to 0} Q(j\omega) = 1$

Also, from (3.9) and (3.10) it is derived that-

$$\lim_{\omega\to 0} T_{ry}(j\omega) = G_{n-}(j\omega) \tag{3.12}$$

$$\lim_{\omega\to 0} T_{dy}(j\omega) = 0 \tag{3.13}$$

From (3.12) it can be concluded that in low frequency domain the DOB characteristics are same as that of $G_{n-}(s)$. And from (3.13) it can be concluded that disturbances in low frequency ranges have been attenuated completely.

Example:

Suppose transfer functions $G_{n-}(s), G_{n+}(s), D(t)$ are taken as

$$G_{n-}(s) = \frac{0.8(1+0.1s)}{(1.5s+1)(3s+1)}\ , \ G_{n+}(s) = \frac{(1-0.1s)}{(1+0.1s)},\ \text{D(t)=3, for t}\geq 2.$$

Q(s) is taken as first order LPF so that $Q(s)G_n^{-1}$ is realizable

$$\frac{1}{\lambda s + 1}$$

The response curves under different filter parameters shown below

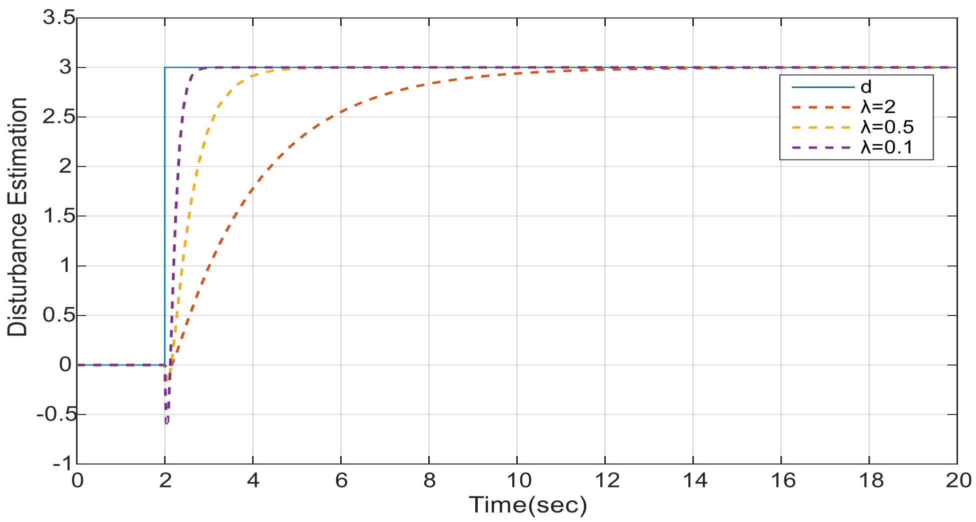

Fig.3.10- Disturbance estimation plots for different λ values

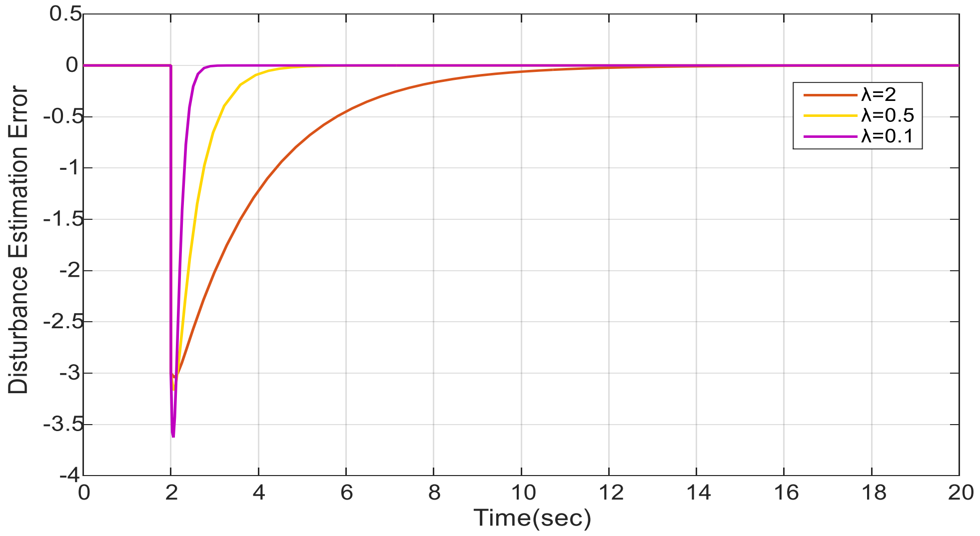

Fig.3.11- Disturbance estimation error plots for different λ values

Observations:

For using small values of λ the disturbance estimation can be done faster and more precisely than using higher values of λ. Like in this fig.4 using $\lambda = 2$ the estimation is showing sluggish response. Using $\lambda = 0.5$ the estimation is done faster than before. For $\lambda = 0.1$ the response is fastest. At t=2 sec the error is maximum for $\lambda = 0.1$, then it decays to zero quickly, whereas for $\lambda = 2$, the error is minimum at t=2 sec but it decays to sluggishly.

Chapter 4

Study of Motion control System

4.1 Introduction:

In this chapter, the stability, performance and robustness of DOB based motion control system [24] has been analysed in detail and validated. But, in this thesis only position control system is the main focus of study. DOB was first proposed by K. Ohnishi to improve motion control system performance, after that it has been used widely in several motion control system such as- robotics, industrial automation, servo-system etc. due to its simple structure and an efficient tool to handle disturbances. Being a 2-DOF controller, DOB suppresses the disturbances in inner-loop, then controllers can be implemented in outer-loop to achieve performance goals like position, force based on nominal plant model.

Although there are many motors but we will be dealing with dc motor for its wide range of application in industry, simplicity and easily controllable design. At first, the dynamic equation of dc motor has been represented in BD. Then DOB has been applied to it with PD controller in outer loop. Then the design constraints of DOB and nominal plant parameters like inertia, torque co-efficient etc are derived analytically by considering the practical constraints of DOB based motion control systems. How DOB can be used as lag-lead compensator that is also shown. How the stability and robustness is dependent on plant parameters that has been described in details along with the trade-off between stability and robustness. Then robust position control has been analysed in detail.

4.2 System description:

Motion control theory has been described in earlier chapter. It usually includes control of position/velocity and acceleration but acceleration control has its limitations in many applications. Motion control can provide basic and advance functionality in automated control system. AT starting, motion control had its own controller and application software with motion-control algorithms to get the work done. But now-a-days much of the motion control can be performed in the main control-system controller by careful selection of the controller, but motion still requires specialty amplifiers, drives, motors, position feedback devices and precision mechanical linkage or actuators.

4.2.1 Block diagram representation and time response:

Here dc servomotor model has been described along with its block diagram and time response. The dynamic equation of dc motor can be written as

$$\tau_m - \tau_l = J\ddot{q} \tag{4.1}$$

τ_m is the motor generated torque, τ_l is the load torque J is the inertia and $\ddot{q}$ is the motor acceleration.

Again,

$$\tau_m = K_t I_a \tag{4.2}$$

Where K_t is uncertain torque co-efficient and I_a is armature current of motor which is taken as reference input.

In s domain the equation (4.1) becomes

$$K_t I_a - \tau_l = J s^2 q \tag{4.3}$$

So

$$q = \frac{(K_t I_a - \tau_l)}{J s^2} \tag{4.4}$$

Block diagram of the above equation is shown below

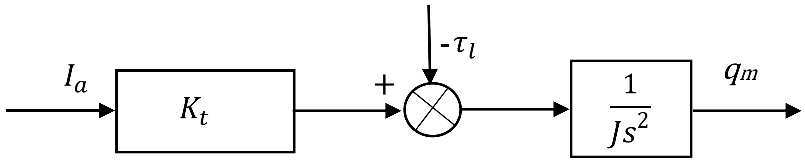

Fig. 4.1- Block diagram of dc servo motor

I_a has been taken as step input of 0.11 amp, $K_t = 5$ Nm/A, $J = 0.1$ kgm^2. Sinusoidal disturbance of unit amplitude has been applied at t=2sec.

The time response plot of the above figure has been shown both in presence of load torque and absence of load torque.

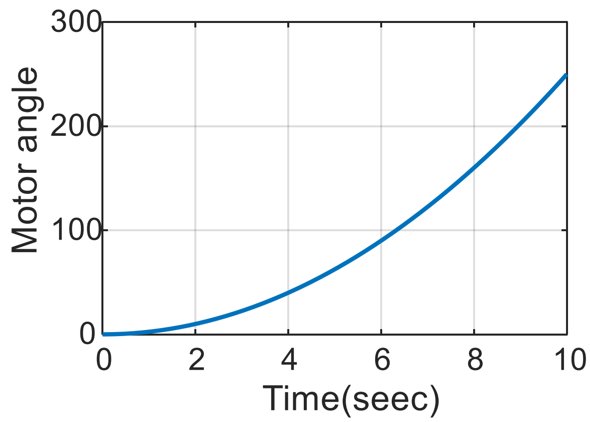

Fig. 4.2- Motor output angle in absence of disturbance

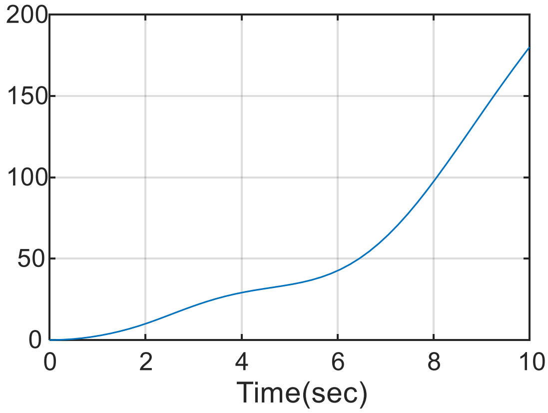

Fig. 4.3- Motor output angle in presence of disturbance

4.3 DOB based robust motion control system:

A block diagram of DOB based robust motion control system is shown below

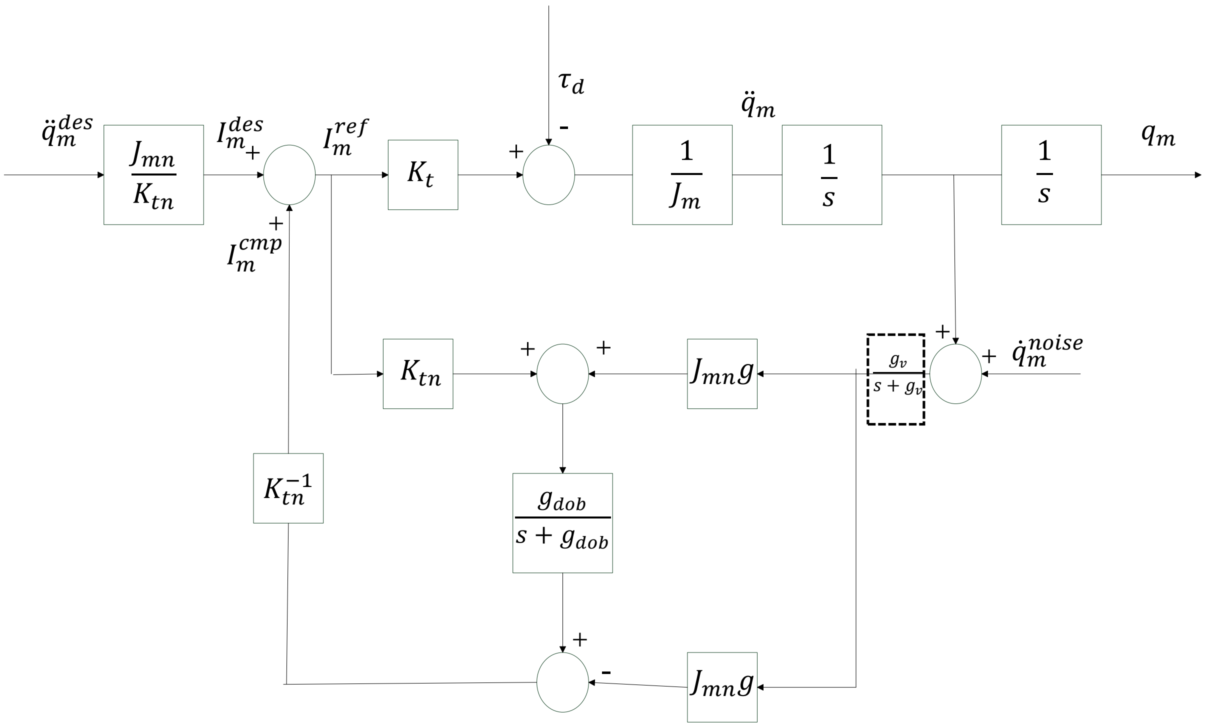

Fig. 4.4- Block diagram of a DOB based motion control system considering ideal velocity estimation, dotted transfer function is considered for practical velocity estimation [24]

DOB estimates external disturbances and plant uncertainties, such as gravity, friction, inertia variation, etc., in the inner-loop then the estimated disturbances is fed back achieving robustness for the motion control system.

The dynamic equation of a DOB based dc servo motor can be written from figure as

$$K_{tn}I_m^{ref} - \tau_m^{dis} = J_m\ddot{q}_m \tag{4.5}$$

So,

$$K_{tn}I_m^{ref} - J_{mn}\ddot{q}_m = \tau_m^{dis} = \tau_m^d + \Delta J_m\ddot{q}_m - \Delta K_t I_m \tag{4.6}$$

Where, $\Delta J_m = J_m - J_{mn}$ which denotes the inertia variation and $\Delta K_t = K_t - K_{tn}$ denotes torque co-efficient variation.

$$\tau_m^d = \tau_m^{load} + \tau_m^{frc} + \tau_m^{int} \tag{4.7}$$

When parameter variations are zero,

$$\tau_m^{dis} = \tau_m^d \tag{4.8}$$

As the estimation includes double derivative of position seen from equation (4.5) it introduces high frequency noise. Hence, a LPF is used to filter out the noise and DOB is derived with LPF. Velocity information is taken by taking derivative of position and a LPF.

$$\hat{\tau}_m^{dis} = \left(\frac{g_{dob}}{s + g_{dob}}\right) \tau_m^{dis} \tag{4.9}$$

Putting τ_m^{dis} from equation (4.6)

$$\hat{\tau}_m^{dis} = \left(\frac{g_{dob}}{s + g_{dob}}\right) \left(K_{tn} I_m^{ref} - J_{mn} \ddot{q}_m\right)$$

$$\text{Or, } \hat{\tau}_m^{dis} = \left(\frac{g_{dob}}{s+g_{dob}}\right) \left(K_{tn} I_m^{ref} - J_{mn} s \dot{q}_m\right)$$

$$\text{Or, } \hat{\tau}_m^{dis} = \left(\frac{g_{dob}}{s+g_{dob}}\right) \left(K_{tn} I_m^{ref} + g_{dob} J_{mn} \dot{q}_m\right) - g_{dob} J_{mn} \dot{q}_m$$

This is how $\hat{\tau}_m^{dis}$ is obtained analytically.

The compensation current I_{cmp} is calculated from estimated disturbance as

$$I_{cmp} = \frac{\hat{\tau}_m^{dis}}{K_{tn}}$$

This compensated current is fed back to achieve robust control.

From fig. (4.4) it is seen that DOB based motion control system has MISO structure. Its transfer function can be written as

$$\ddot{q}_m = \alpha \frac{(s + g_{dob})}{(s + \alpha g_{dob})} \ddot{q}_m^{des} - \frac{1}{J_m} T_{DOB}^{SEN} + T_{DOB}^{CoSEN} s \dot{q}_m^{noise} \tag{4.10}$$

$$\text{where } T_{DOB}^{SEN} = \frac{1}{1+L_{DOB}(s)}, T_{DOB}^{CoSEN} = \frac{L_{DOB}(s)}{1+L_{DOB}(s)},$$

$$\text{and } L_{DOB}(s) = \alpha \frac{g_{dob}}{s}, \text{ where } \alpha = \frac{J_{mn} K_t}{J_m K_{tn}}.$$

Fig. (4.4) used as conventional analysis but it is impractical if velocity estimation is assumed to be ideal. Precise velocity measurement is needed for DOB. Hence a LPF is used to cancel out the noise in velocity measurement in pre-determined BW , the LPF is shown as dotted block.

In fig. (4.4) g_v denotes cut-off frequency of velocity measurement. Transfer function of practical DOB based motion control system is

$$\ddot{q}_m = \alpha \frac{(s + g_{dob})(s + g_v)}{(s^2 + g_v s + \alpha g_v g_{dob})} \ddot{q}_m^{des} - \frac{1}{J_m} T_{DOB}^{SEN} + T_{DOB}^{CoSEN} s \dot{q}_m^{noise} \tag{4.11}$$

T_{DOB}^{SEN} and T_{DOB}^{CoSEN} are same as above but

$$L_{DOB}(s) = \alpha \frac{g_v g_{dob}}{s(s + g_v)}$$

From equation (4.10), (4.11) it can be said that by changing the α value DOB can be used as phase lag/lead compensator. If α>1, then it is phase lead compensator and if α<1 it works as phase lag compensator. The stability and performance can be improved by increasing phase lead. The upper bound of α will be derived in later section.

4.3.1 Transfer function derivation:

Case 1- when g_v is infinite:

To evaluate $\frac{\ddot{q}_m}{\ddot{q}_m^{des}}$, τ_m^d and $\dot{q}_m^{noise}$ are taken as zero input. The BD shown below

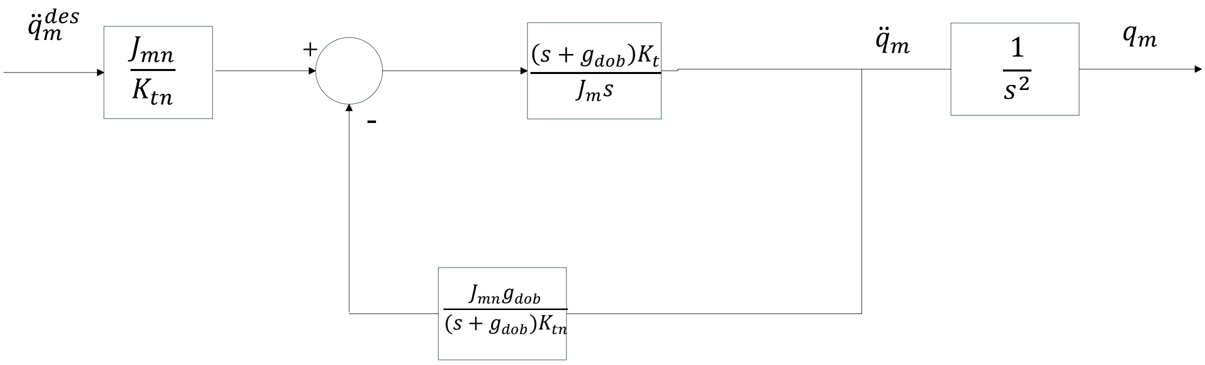

Fig. 4.5- Simplified BD of fig. (4.4)

$$\frac{\ddot{q}_m}{\ddot{q}_m^{des}} = \frac{J_{mn}}{K_{tn}}\left[\frac{\frac{(s+g_{dob})K_t}{J_m s}}{1+(\frac{s+g_{dob}}{J_m s})K_t(\frac{J_{mn}g_{dob}}{s+g_{dob}})\left(\frac{1}{K_{tn}}\right)}\right]$$

$$= \frac{J_{mn}}{K_{tn}}\left[\frac{(s+g_{dob})K_t K_{tn}}{J_m K_{tn} s + J_{mn} g_{dob} K_t}\right]$$

$$= \frac{J_{mn}K_t}{K_{tn}J_m}\left[\frac{(s+g_{dob})}{s+\frac{J_{mn}K_t}{K_{tn}J_m}g_{dob}}\right]$$

$$\frac{\ddot{q}_m}{\ddot{q}_m^{des}} = \alpha\left(\frac{s+g_{dob}}{s+\alpha g_{dob}}\right)$$

To evaluate sensitivity transfer function i.e. T_{DOB}^{SEN} and T_{DOB}^{CoSEN} we need to calculate $L_{DOB}(s)$ i.e. GH(s) for easier calculation. The simplified BD shown below

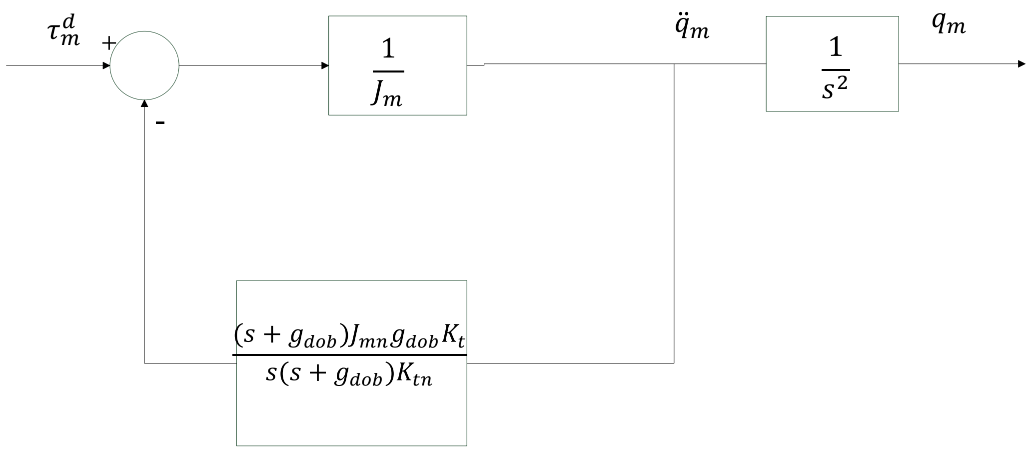

Fig. 4.6- Simplified block diagram of fig. (4.4)

Here $G(s) = \frac{1}{J_m}$ and

$H(s)$ is calculated as follows

$$H(s) = (\frac{s + g_{dob}}{s})K_t(\frac{J_{mn}g_{dob}}{s + g_{dob}})\left(\frac{1}{K_{tn}}\right)$$

So,

$$L_{DOB}(s) = GH(s) = \frac{J_{mn}K_t}{J_m K_{tn} s}$$

$$L_{DOB}(s) = \alpha \frac{g_{dob}}{s}$$

Hence we get,

$$T_{DOB}^{SEN} = \frac{1}{1 + L_{DOB}(s)}$$

$$= \frac{1}{1 + \alpha \frac{g_{dob}}{s}}$$

$$= \frac{s}{s + \alpha g_{dob}}$$

And,

$$T_{DOB}^{CoSEN} = \frac{L_{DOB}(s)}{1 + L_{DOB}(s)}$$

$$= \frac{\alpha g_{dob}}{s + \alpha g_{dob}}$$

Case 2- when g_v is finite:

From fig. (4.6), $L_{DOB}(s)$ can be derived by multiplying the feedback block by $\left(\frac{g_v}{s+g_v}\right)$

$$L_{DOB}(s) = G(s) * H(s) = \frac{1}{J_m} * \left(\frac{s + g_{dob}}{s}\right) K_t \left(\frac{J_{mn} g_{dob}}{s + g_{dob}}\right) \left(\frac{1}{K_{tn}}\right) * \left(\frac{g_v}{s + g_v}\right)$$

$$\text{Or,} L_{DOB}(s) = \alpha \frac{g_{dob}}{s} * \left(\frac{g_v}{s+g_v}\right)$$

So,

$$T_{DOB}^{SEN} = \frac{1}{1 + L_{DOB}(s)}$$

$$= \frac{1}{1 + \alpha \frac{g_{dob}}{s} \left(\frac{g_v}{s + g_v}\right)}$$

$$= \frac{s(s + g_v)}{s(s + g_v) + \alpha g_v g_{dob}}$$

And,

$$T_{DOB}^{CoSEN} = \frac{L_{DOB}(s)}{1 + L_{DOB}(s)}$$

$$= \frac{\alpha g_v g_{dob}}{s(s + g_v) + \alpha g_v g_{dob}}$$

$\frac{\ddot{q}_m}{\ddot{q}_m^{des}}$ can be derived as

$$\frac{\ddot{q}_m}{\ddot{q}_m^{des}} = \frac{J_{mn}}{K_{tn}} \left[\frac{\frac{(s + g_{dob})K_t}{J_m s}}{1 + \left(\frac{s + g_{dob}}{J_m s}\right) K_t \left(\frac{J_{mn} g_{dob}}{s + g_{dob}}\right) \left(\frac{1}{K_{tn}}\right) \left(\frac{g_v}{s + g_v}\right)} \right]$$

$$= \frac{J_{mn}}{K_{tn}} \left[\frac{(s + g_{dob})(s + g_v) K_t K_{tn}}{J_m K_{tn} s(s + g_v) + J_{mn} g_v g_{dob} K_t} \right]$$

$$= \frac{J_{mn}K_t}{K_{tn}J_m}\left[\frac{(s+g_{dob})(s+g_v)}{s(s+g_v)+\frac{J_{mn}K_t}{K_{tn}J_m}g_v g_{dob}}\right]$$

$$\frac{\ddot{q}_m}{\ddot{q}_m^{des}} = \alpha\frac{(s+g_v)(s+g_{dob})}{s^2+g_v s+\alpha g_v g_{dob}}$$

4.3.2 Robustness analysis:

The two equations (4.10) and (4.11) may seem similar but when velocity is measured using LPF robustness of a DOB based motion control system changes significantly. Depending on g_v value relative degree of $L_{DOB}(s)$ changes. When g_v is infinite it is 1 and 2 when g_v is finite. According to bode integral theorem, T_{DOB}^{SEN} can not be shaped properly is relative degree of $L_{DOB}(s)$ is higher than 1.The peak of T_{DOB}^{SEN}increases at higher frequencies. So, α and g_{dob} can not be increased freely due to robustness constraint. This constraint can be derived analytically shown below

The characteristic polynomial of T_{DOB}^{SEN} or T_{DOB}^{CoSEN} can be written as–

$$C_h(s) = s^2 + g_v s + \alpha g_v g_{dob} \tag{4.12}$$

Applying $g_v = \kappa g_{dob}$ we get

$$C_h(s) = s^2 + \kappa g_{dob} s + \alpha\kappa g_{dob}^2 \tag{4.13}$$

Natural frequency $\omega_n = \sqrt{\alpha\kappa}g_{dob}$, and damping co-efficient $\zeta = 0.5\sqrt{\alpha^{-1}\kappa}$

To suppress the peak ofT_{DOB}^{SEN} or T_{DOB}^{CoSEN}, ζ value is taken as

$$\zeta \geq 0.707$$

Then we get

$$\alpha g_{dob} \leq \frac{g_v}{2} \tag{4.14}$$

The equation (4.14) shows a new practical design constraint. α and g_{dob} are limited by this constraint when we consider imperfect velocity estimation. The robustness of a DOB can be improved by increasing the lower constraint of ϵ but, the upper bound of α and g_{dob} become more severe, this means the stability and performance deteriorate. Consequently, there is a trade-off between the robustness, stability, and performance in DOB based motion control systems. Bode plot has been done on sensitivity and co- sensitivity functions to represent graphically the robustness constraint of DOB based motion control. The figures have been shown below

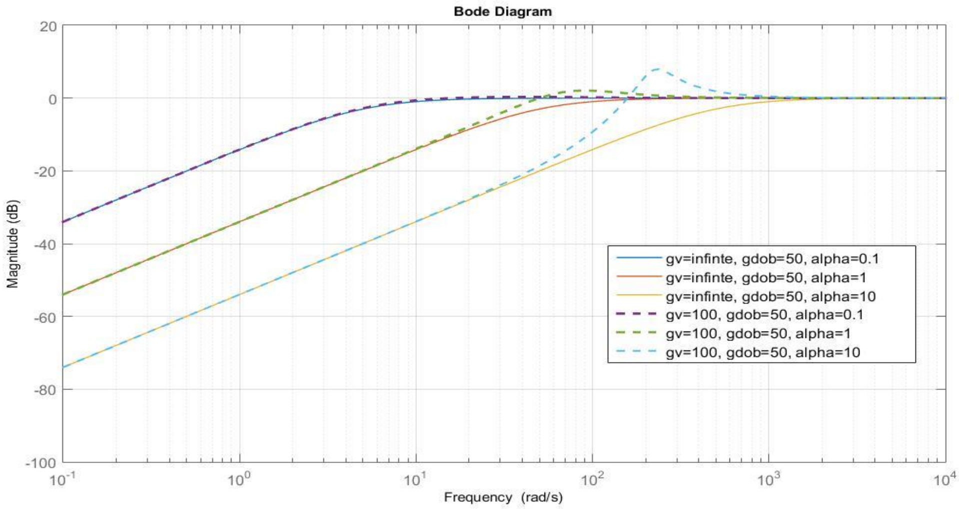

Fig. 4.7- Sensitivity function for different values of α

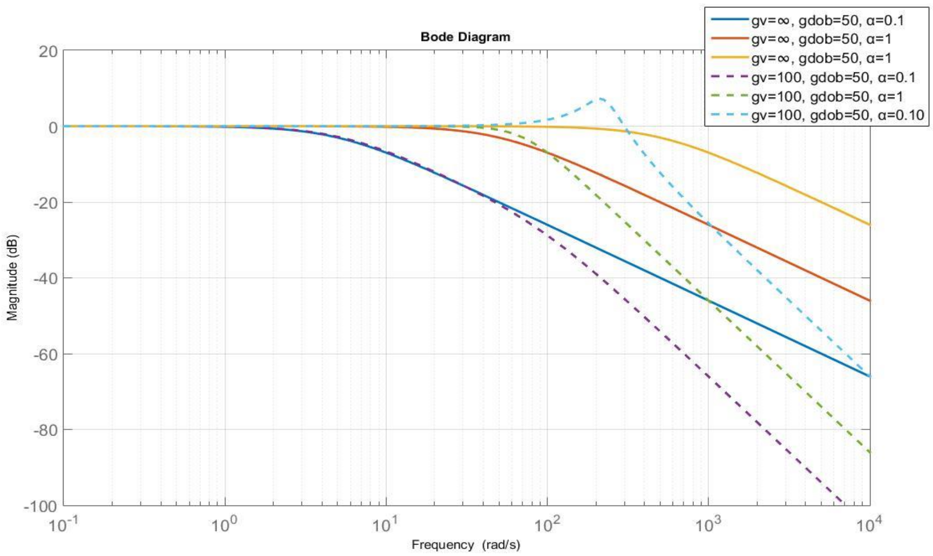

Fig. 4.8- Co-Sensitivity function for different values of α

Observation from the plots:

It is clearly seen that in case of ideal velocity estimation i.e. when g_v is infinite, not only the performance but also the robustness improves, but in reality ideal velocity estimation is not achievable. In case of imperfect velocity estimation the frequency responses of sensitivity and complementary sensitivity function change significantly. A prominent peak has been seen in case of imperfect velocity estimation when α=10 as the condition given in equation (4.14) is not satisfying in this case.

4.3.3 Disturbance estimation:

Disturbance estimation is done without any outer-loop controller and considering parameter uncertainties to be zero. Here, sinusoidal current of magnitude 1A is given at t=0 sec, and sinusoidal disturbance of 1 N-m has been applied, the values $g_{dob} = 50$ rad/s, $J_{mn} = 0.1$ kg-m^2, $K_{tn} = 5$ N-m/A have been taken. The fig. (4.9) represents the applied and estimated disturbance.

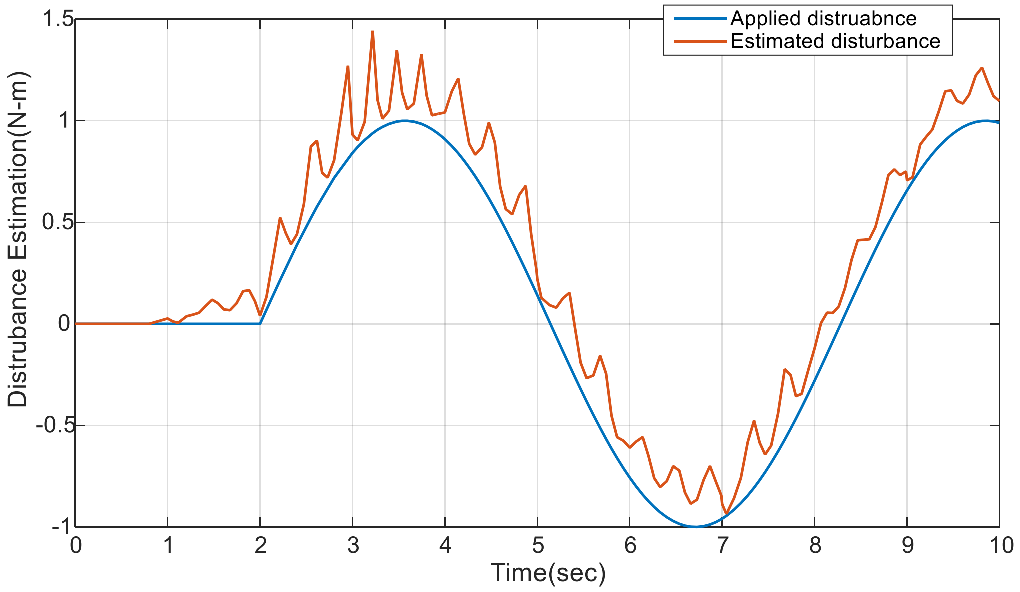

Fig. 4.9- Disturbance estimation plot considering only inner-loop

4.4 DOB based robust Position Control System:

The BD of DOB based robust position control system shown below

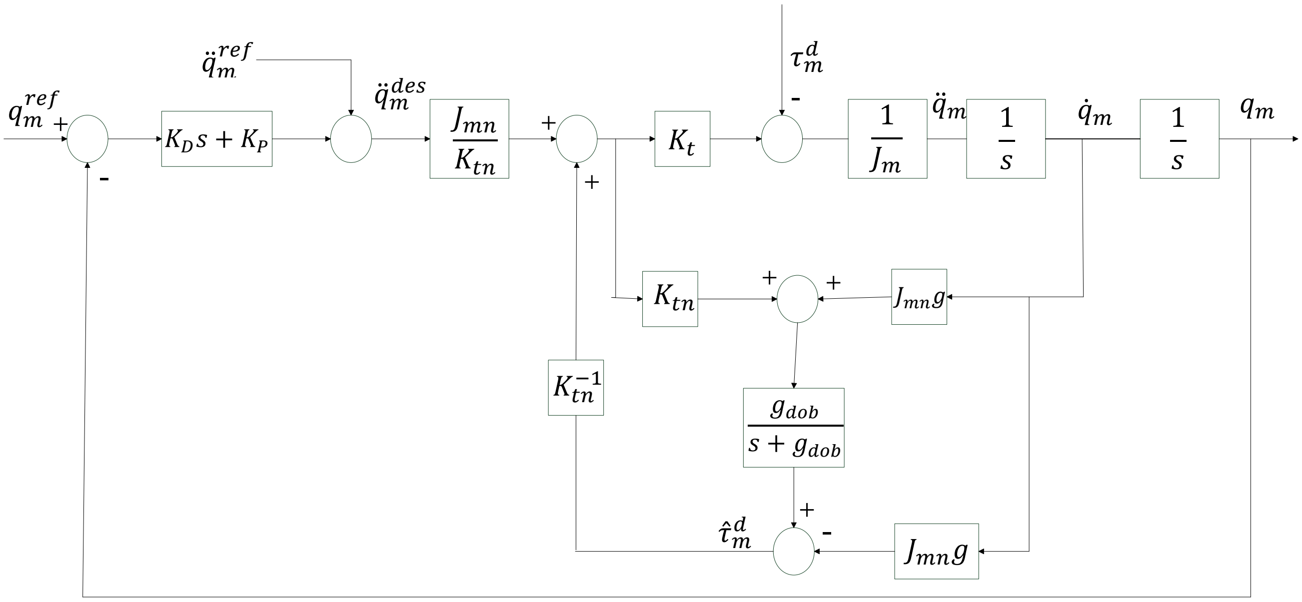

Fig. 4.10- Block diagram of a DOB based robust position control system [24]

Here q_m^{ref} and $\ddot{q}_m^{ref}$ denotes angle/position and acceleration reference inputs respectively. A PD controller is used in outer loop to achieve performance goals. K_D and K_P is derivative and proportional control gain respectively. The transfer function between $\ddot{q}_m^{ref}$ and q_m^{ref} derived from fig. (4.10) can be written as

$$\frac{\ddot{q}_m}{\ddot{q}_m^{ref}} = \frac{\alpha s^2(s+g_{dob})}{s^2(s+\alpha g_{dob}) + \alpha(s+g_{dob})(K_D s + K_P)} \tag{4.15}$$

When g_v is infinite. And,

$$\frac{\ddot{q}_m}{\ddot{q}_m^{ref}} = \frac{\alpha s^2(s+g_v)(s+g_{dob})}{s^2(s^2+g_v s+\alpha g_v g_{dob}) + \alpha(s+g_v)(s+g_{dob})(K_D s + K_P)} \tag{4.16}$$

When g_v is finite.

4.4.1 Transfer function derivation:

Case 1: When g_v is infinite:

From equation (4.10) it is found that

$$\frac{\ddot{q}_m}{\ddot{q}_m^{des}} = \alpha\left(\frac{s+g_{dob}}{s+\alpha g_{dob}}\right)$$

The simplified BD of fig.(4.10) has shown below

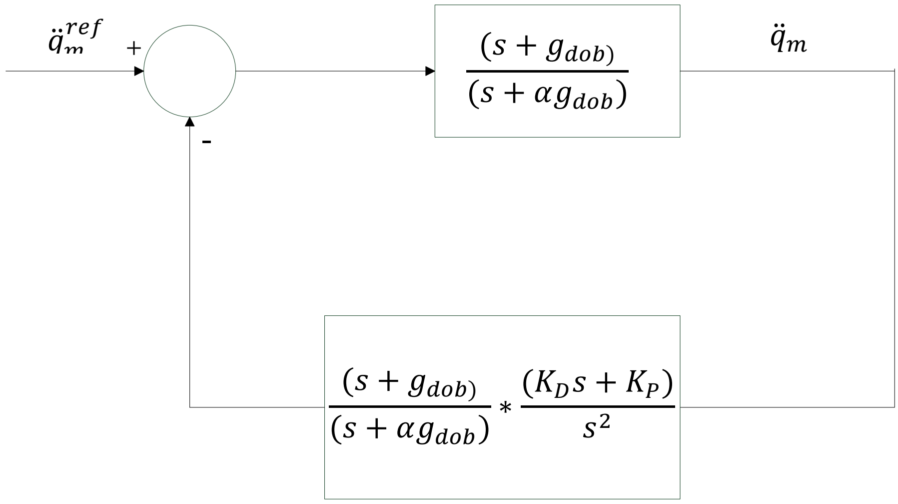

Fig. 4.11 – Simplified block diagram of fig. (4.9)

$$\frac{\ddot{q}_m}{\ddot{q}_m^{ref}} = \frac{\alpha\left(\frac{s+g_{dob}}{s+\alpha g_{dob}}\right)}{1+\alpha\left(\frac{s+g_{dob}}{s+\alpha g_{dob}}\right)\left(\frac{K_D s+K_P}{s^2}\right)}$$

$$\frac{\ddot{q}_m}{\ddot{q}_m^{ref}} = \frac{\alpha s^2(s+g_{dob})}{s^2(s+\alpha g_{dob})+\alpha(s+g_{dob})(K_D s+K_P)} \quad (4.17)$$

Case 2- when g_v is finite:

$$\frac{\ddot{q}_m}{\ddot{q}_m^{ref}} = \frac{\alpha\frac{(s+g_v)(s+g_{dob})}{s^2+g_v s+\alpha g_v g_{dob}}}{1+\alpha\frac{(s+g_v)(s+g_{dob})}{(s^2+g_v s+\alpha g_v g_{dob})}\left(\frac{K_D s+K_P}{s^2}\right)}$$

$$\frac{\ddot{q}_m}{\ddot{q}_m^{ref}} = \frac{\alpha s^2(s+g_v)(s+g_{dob})}{s^2(s^2+g_v s+\alpha g_v g_{dob})+\alpha(s+g_v)(s+g_{dob})(K_D s+K_P)} \quad (4.18)$$

It is obvious from the equation (4.18) that characteristic functions are dependent on g_{dob}, g_v, α K_P, K_D.

4.4.2 Stability analysis:

Let us consider the equation (4.15) by using RH criterion to perform stability analysis we get

$$\alpha^{-1} < 1 + g_{dob}\frac{K_D}{K_P} + \frac{K_D}{g_{dob}} + \frac{{K_D}^2}{K_P} \tag{4.19}$$

This equation (4.19) is the stability criteria. From this equation it can be concluded that stability of robust position control can be improved by increasing the value of α and g_{dob}. But from the robustness analysis i.e. from eq (4.14) it has been observed that α and g_{dob} can not be freely increased. This is the trade-off between robustness and stability.

Generally it is assumed that robustness and performance can be controlled in inner and outer loop separately, but it is not true indeed. The robustness depends on outer loop as well. It will be clarified by deriving T_{PC}^{SEN} and T_{PC}^{CoSEN}.

$$T_{PC}^{SEN} = \frac{1}{1 + L_{PC}(s)} \tag{4.20}$$

$$T_{PC}^{CoSEN} = \frac{L_{PC}(s)}{1 + L_{PC}(s)} \tag{4.21}$$

$$L_{PC}(s) = \alpha\frac{g_{dob}s^2 + (s + g_{dob})(K_D s + K_P)}{s^3} \tag{4.22}$$

When g_v is infinite, and

$$L_{PC}(s) = \alpha\frac{g_{dob}g_v s^2 + (s + g_{dob})(s + g_v)(K_D s + K_P)}{s^3(s + g_v)} \tag{4.23}$$

When g_v is finite.

From equations (4.20) and (4.21) it is observed that increasing the outer loop controller gain leads to more robust system when $\alpha g_{dob} > 0.5 g_v$ .Still, inner loop becomes sensitive to high frequency noises. Again, increasing outer loop controller gain has several disadvantages like energy consumption, vibration due to high frequency dynamics etc.

Derivation of $L_{PC}(s)$:

Case1- when g_v is infinite:

The characteristic equation from (4.15) we get

$$C_h(s) = s^2(s + \alpha g_{dob}) + \alpha(s + g_{dob})(K_D s + K_P)$$

By rearranging we get

$$C_h(s) = s^3 + \alpha[g_{dob}s^2 + (s + g_{dob})(K_D s + K_P)]$$

$$s^3[1 + \frac{\alpha\{g_{dob}s^2 + (s + g_{dob})(K_D s + K_P)\}}{s^3}$$

So, loop transfer function

$$L_{PC}(s) = \frac{\alpha[g_{dob}s^2 + (s + g_{dob})(K_D s + K_P)]}{s^3}$$

Case2- when g_v is finite:

The characteristic equation from (4.16) we get

$$C_h(s) = s^2(s^2 + g_v s + \alpha g_v g_{dob}) + \alpha(s + g_v)(s + g_{dob})(K_D s + K_P)$$

By rearranging we get

$$C_h(s) = s^3(s + g_v) + \alpha[g_v g_{dob}s^2 + (s + g_v)(s + g_{dob})(K_D s + K_P)]$$

$$s^3(s + g_v)[1 + \frac{\alpha\{g_v g_{dob}s^2 + (s + g_v)(s + g_{dob})(K_D s + K_P)\}}{s^3(s + g_v)}$$

So, loop transfer function

$$L_{PC}(s) = \frac{\alpha[g_v g_{dob}s^2 + (s + g_v)(s + g_{dob})(K_D s + K_P)]}{s^3(s + g_v)}$$

4.5 Simulations:

In this section, simulation results have been given with detailed analysis. The values of the variables taken for this simulations shown below [26]

J_{mn}= 0.1 kgm^2, K_{tn}= 5 Nm/A, K_P= 900, K_P=100.

The simulation starts by considering robustness of position control system. The following figure describes outer-loops' co-sensitivity function frequency response i.e. T_{PC}^{CoSEN} when PD controller is used in outer-loop. Inner-loop frequency responses has already been shown in previous section.

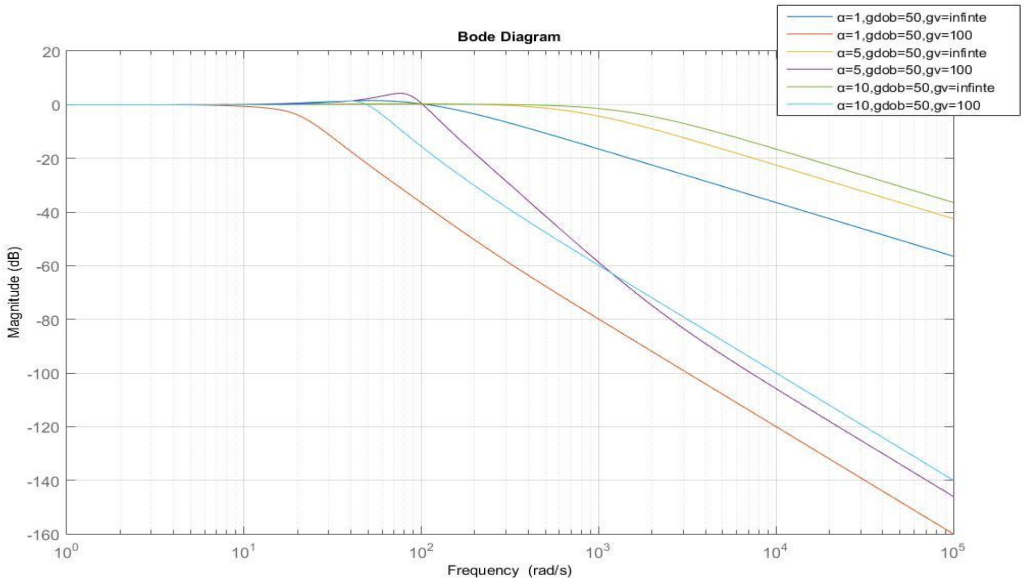

Fig. 4.12- Outer-loop Co-Sensitivity function frequency responses for different values of α

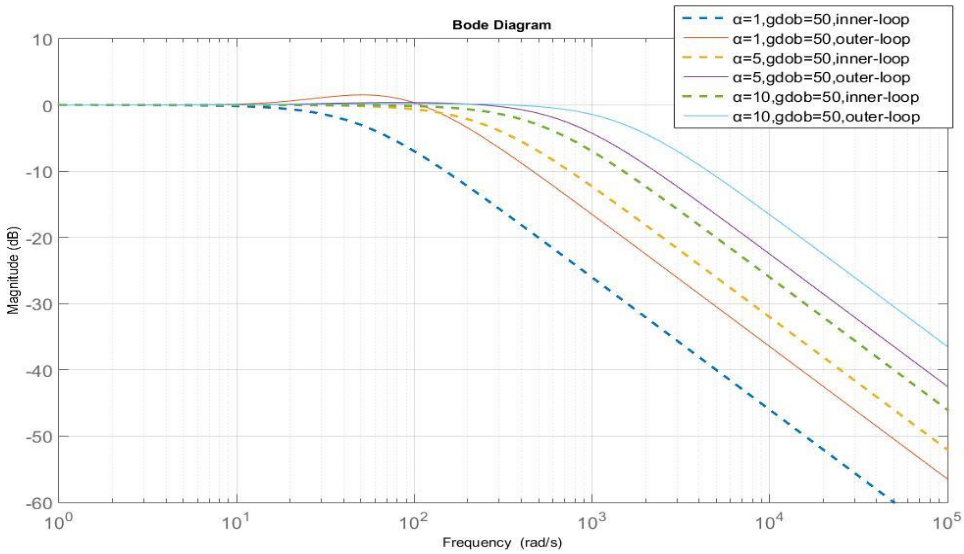

Fig. 4.13- Inner loop and outer-loop Co-sensitivity function frequency responses

From the fig. (4.12) it can be said that for imperfect velocity estimation the bandwidth is lower than that of perfect velocity estimation. Also outer loop controller can improve robustness as shown in fig. (4.13). Though the robustness has increased for outer-loop, DOB becomes more sensitive to high frequency noises in inner-loop as αg_{dob} is increased.

Now, stability of position control has been discussed. The following fig. (4.14) is the root locus plotted w.r.t α when $g_{dob} = 500$ rad/s.

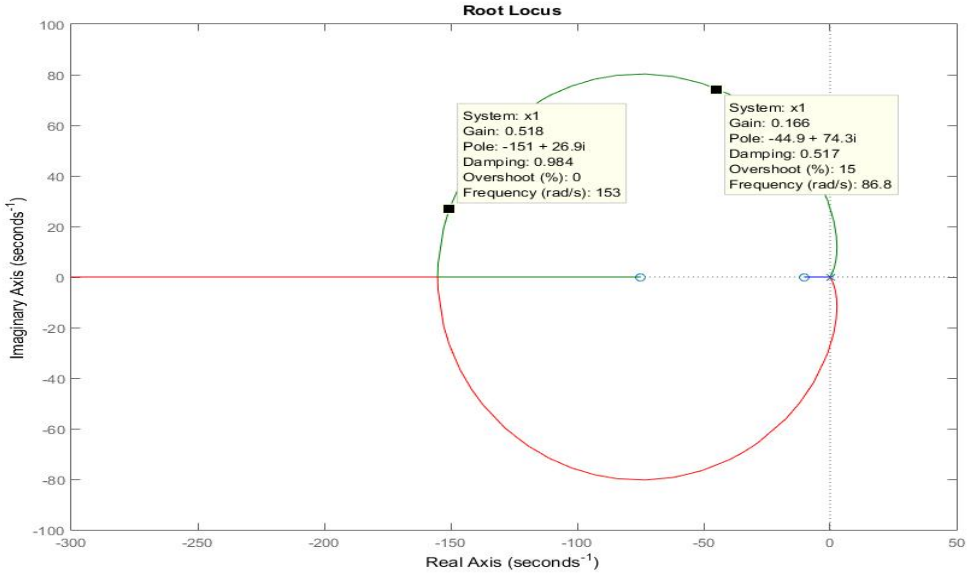

Fig. 4.14- Root locus plot showing stability of position control system

The figure clearly describes that on increasing the α, i.e. the gain value, the plot is shifting towards left, thereby increasing stability. Though the increment is limited by robustness constraint as described earlier. So, the trade-off between robustness and stability has been described analytically and graphically.

The position response is shown below when sinusoidal angle reference and sinusoidal disturbance has been applied at t=0 and t=2 respectively

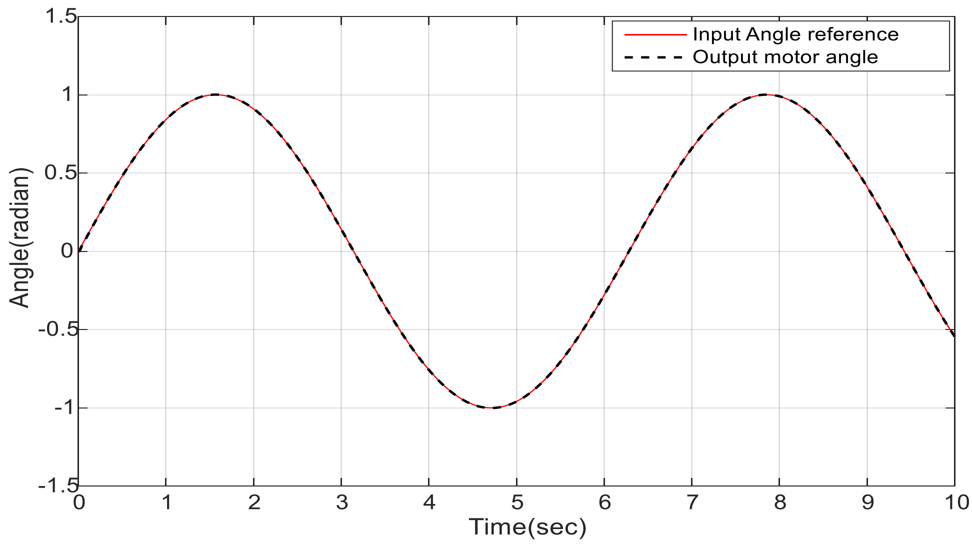

Fig.4.15- Position Control response when sinusoidal input is applied at t=0 and sinusoidal disturbance at t=2 sec

The position tracking error plots with different inputs have been shown in chapter 6.

Chapter 5

Proposed PID Controller and DOB

5.1 Introduction:

In this chapter, DOB based motion control system with PID controller has been discussed in details. It starts with the design constraints of DOB and nominal plant parameters like inertia, torque co-efficient etc., these are derived analytically by considering the practical constraints of DOB based motion control systems, the criteria is similar as shown in chapter 4. How the stability and robustness is dependent on plant parameters that has been described in details along with the trade-off between stability and robustness. PID controller tuning has also been discussed. Then PID controller and DOB based robust position control has been analysed in detail.

5.2 DOB based motion control system:

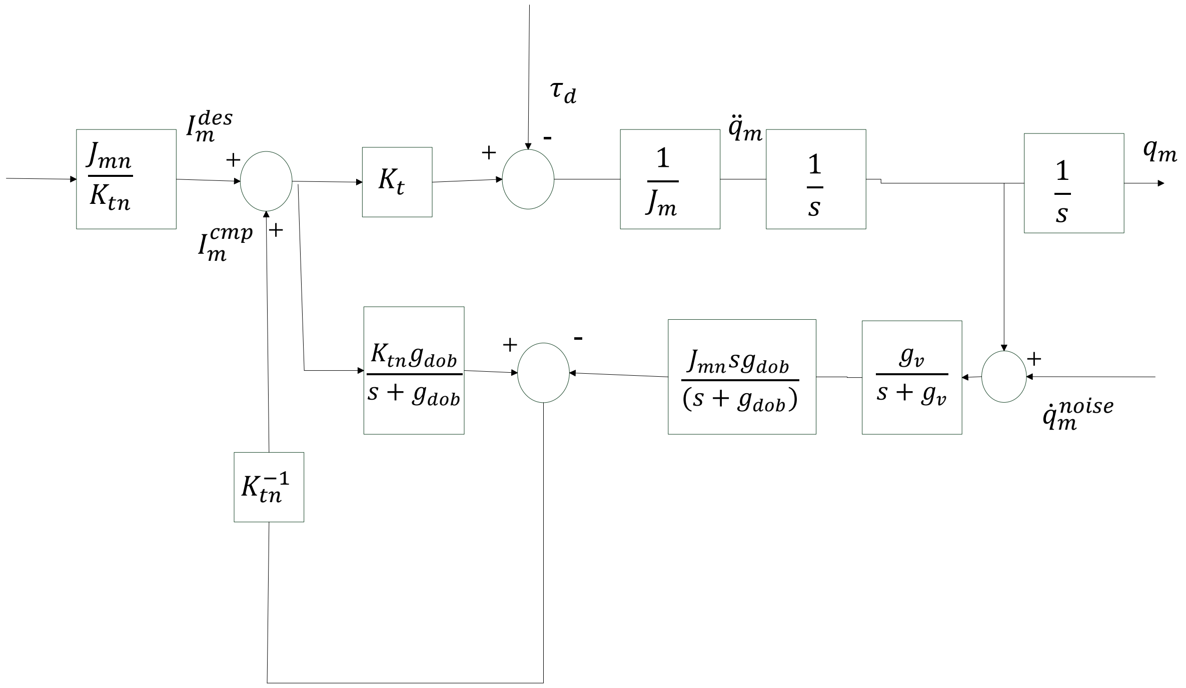

Fig. 5.1- Servo motor system with DOB

From fig. (5.1) its transfer function can be written as

$$\ddot{q}_m = \alpha \frac{(s+g_{dob})}{(s+\alpha g_{dob})} \ddot{q}_m^{des} - \frac{1}{J_m} T_{DOB}^{SEN} + T_{DOB}^{CoSEN} s \dot{q}_m^{noise} \tag{5.1}$$

where $T_{DOB}^{SEN} = \frac{G_n(s)[1-Q(s)]}{G_n(s)[1-Q(s)]+G_p(s)Q(S)}$,

$$T_{DOB}^{CoSEN} = \frac{G_p(s)Q(S)}{G_n(s)[1-Q(s)]+G_p(s)Q(S)},$$

and $G_n(s) = \frac{K_{tn}}{Js}$, where $Q(s) = \frac{g_{dob}}{s+g_{dob}}$.

Fig. (5.1) is used as practical block diagram. Precise velocity measurement is needed for DOB. Hence a LPF is used to cancel out the noise in velocity measurement in pre-determined BW.

In fig. (5.1) g_v denotes cut-off frequency of velocity measurement. Transfer function of practical DOB based motion control system is

$$\ddot{q}_m = \alpha \frac{(s+g_{dob})(s+g_v)}{(s^2+g_v s+\alpha g_v g_{dob})}\ddot{q}_m^{des} - \frac{1}{J_m}T_{DOB}^{SEN} + T_{DOB}^{CoSEN} s\dot{q}_m^{noise} \tag{5.2}$$

$$T_{DOB}^{SEN} = \frac{1}{1+L_{DOB}(s)}$$

$$T_{DOB}^{CoSEN} = \frac{L_{DOB}(s)}{1+L_{DOB}(s)}$$

Where, $L_{DOB}(s) = \alpha \frac{g_v g_{dob}}{s(s+g_v)}$

From equation (5.1), (5.2) it can be said that by changing the α value DOB can be used as phase lag/lead compensator. If α>1, then it is phase lead compensator and if α<1 it works as phase lag compensator. The stability and performance can be improved by increasing phase lead. The upper bound of α will be derived in later section.

5.2.1 Transfer function derivation:

Case 1- when when g_v is infinite:

To evaluate $\frac{\ddot{q}_m}{\ddot{q}_m^{des}}$, τ_m^d and $\dot{q}_m^{noise}$ are taken as zero input. The simplified block diagram is same as fig. (4.5). So, from chapter 4, equation (4.10) it can be written

$$\frac{\ddot{q}_m}{\ddot{q}_m^{des}} = \alpha\left(\frac{s+g_{dob}}{s+\alpha g_{dob}}\right)$$

To evaluate sensitivity transfer function i.e. T_{DOB}^{SEN} and T_{DOB}^{CoSEN} , the values of $G_n(s), G_p(s), Q(S)$ have been put.

So,

$$T_{DOB}^{SEN} = \frac{\frac{K_{tn}}{J_{mn}s}[1 - \frac{g_{dob}}{s + g_{dob}}]}{\frac{K_{tn}}{J_{mn}s}\left[1 - \frac{g_{dob}}{s + g_{dob}}\right] + \frac{K_t}{J_m s}\left(\frac{g_{dob}}{s + g_{dob}}\right)}$$

$$= \frac{\frac{K_{tn}}{J_{mn}}}{\frac{K_{tn}}{J_{mn}} + \frac{K_t g_{dob}}{J_m s}}$$

$$= \frac{s}{s + \alpha g_{dob}}$$

And,

$$T_{DOB}^{CoSEN} = \frac{\frac{K_t}{J_m s}\left(\frac{g_{dob}}{s + g_{dob}}\right)}{\frac{K_{tn}}{J_{mn}s}\left[1 - \frac{g_{dob}}{s + g_{dob}}\right] + \frac{K_t}{J_m s}\left(\frac{g_{dob}}{s + g_{dob}}\right)}$$

$$= \frac{\frac{K_t g_{dob}}{J_m s}}{\frac{K_{tn}}{J_{mn}} + \frac{K_t g_{dob}}{J_m s}}$$

$$= \frac{\alpha g_{dob}}{s + \alpha g_{dob}}$$

Case 2- when g_v is finite:

As the above expressions for ideal velocity estimation is same, so derivation $L_{DOB}(s)$ is similar to that done in chapter 4. So, directly we can write

$$L_{DOB}(s) = \alpha \frac{g_{dob}}{s} * \left(\frac{g_v}{s + g_v}\right)$$

So,

$$T_{DOB}^{SEN} = \frac{1}{1 + L_{DOB}(s)}$$

$$= \frac{1}{1 + \alpha \frac{g_{dob}}{s}\left(\frac{g_v}{s + g_v}\right)}$$

$$= \frac{s(s + g_v)}{s(s + g_v) + \alpha g_v g_{dob}}$$

And,

$$T_{DOB}^{CoSEN} = \frac{L_{DOB}(s)}{1 + L_{DOB}(s)}$$
$$= \frac{\alpha g_v g_{dob}}{s(s + g_v) + \alpha g_v g_{dob}}$$

Derivation of $\frac{\ddot{q}_m}{\ddot{q}_m^{des}}$ is same as that done in chapter 4. So, it can be written

$$\frac{\ddot{q}_m}{\ddot{q}_m^{des}} = \alpha \frac{(s + g_v)(s + g_{dob})}{s^2 + g_v s + \alpha g_v g_{dob}}$$

5.2.2 Robustness analysis:

The two equations (5.1), (5.2) may seem similar but when velocity is measured using LPF robustness of a DOB based motion control system changes significantly. As discussed in chapter 4, depending on g_v value relative degree of $L_{DOB}(s)$ changes. When g_v is infinite relative degree is 1 and 2 when g_v is finite. According to bode integral theorem, T_{DOB}^{SEN} can not be shaped properly is relative degree of $L_{DOB}(s)$ is higher than 1.The peak of T_{DOB}^{SEN}increases at higher frequencies. So, α and g_{dob} can not be increased freely due to robustness constraint. This constraint can be derived analytically shown below

The characteristic polynomial of T_{DOB}^{SEN} or T_{DOB}^{CoSEN} can be written as–

$$C_h(s) = s^2 + g_v s + \alpha g_v g_{dob} \tag{5.3}$$

Applying $g_v = \kappa g_{dob}$ we get

$$C_h(s) = s^2 + \kappa g_{dob} s + \alpha \kappa g_{dob}^2 \tag{5.4}$$

Natural frequency $\omega_n = \sqrt{\alpha\kappa} g_{dob}$, and damping co-efficient $\zeta = 0.5\sqrt{\alpha^{-1}\kappa}$

To suppress the peak ofT_{DOB}^{SEN} or T_{DOB}^{CoSEN}, ζ value is taken as

$$\zeta \geq 0.707$$

Then we get

$$\alpha g_{dob} \leq \frac{g_v}{2} \tag{5.5}$$

The equation (5.5) shows a new practical design constraint which is same as shown in previous chapter. The robustness of a DOB can be improved by increasing the lower constraint of ζ but, the upper bound of α and g_{dob} become more severe, this means the stability and performance deteriorate. Consequently, there is a trade-off between the robustness, stability, and performance in DOB based motion control systems.

Bode plot has been done on sensitivity and co- sensitivity functions to represent graphically the robustness constraint of DOB based motion control. The figures have been shown below

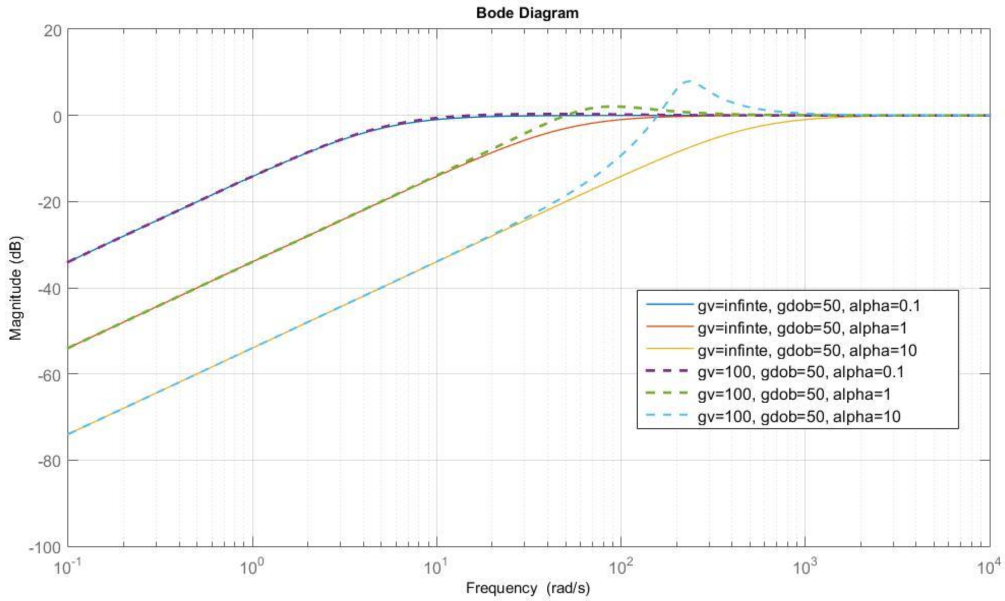

Fig. 5.2- Sensitivity function frequency responses for different values of α

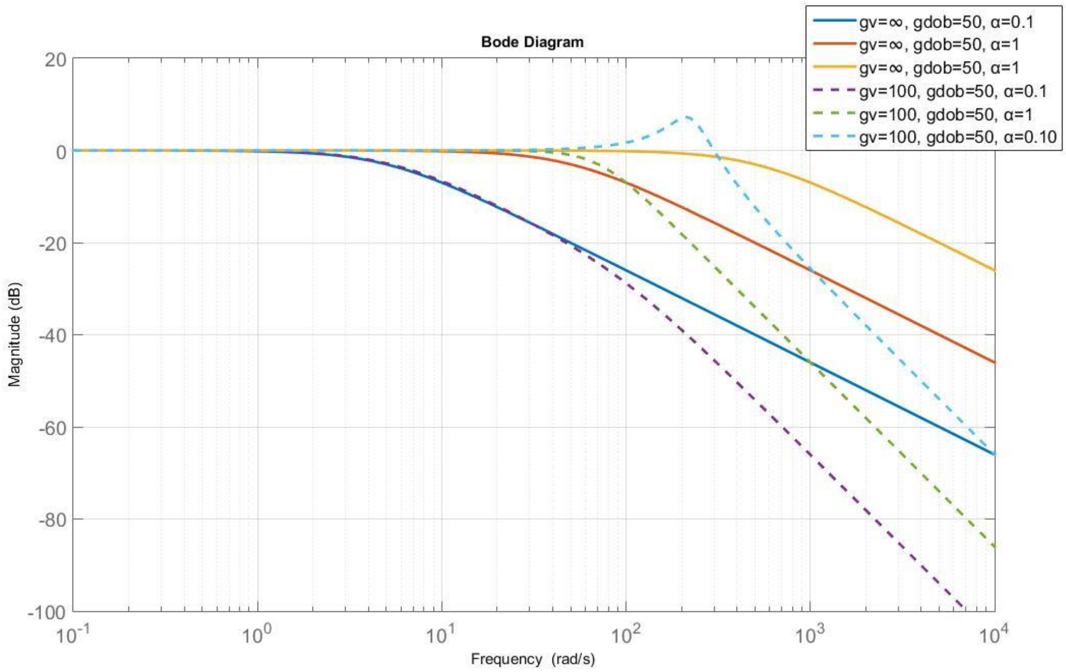

Fig. 5.3- Co-Sensitivity function frequency responses different values of α

Observation from the plots:

It is clearly seen that in case of ideal velocity estimation i.e. when g_v is infinite, not only the performance but also the robustness improves, but in reality ideal velocity estimation is not achievable. In case of imperfect velocity estimation the frequency responses of sensitivity and complementary sensitivity function change significantly. A prominent peak has been seen in case of imperfect velocity estimation when α=10 as the condition given in eq (5.5) is not satisfying in this case. These observations are also same as shown in previous chapter.

The robustness analysis and design constraint here shown is completely same as that of the literature [24].

5.2.3 Disturbance estimation:

Disturbance estimation is done without any outer-loop controller and considering parameter uncertainties to be zero. Here, sinusoidal current of magnitude 1A is given at t=0 sec, and sinusoidal disturbance of 1 N-m has been applied at t=2 sec,the values $g_{dob} = 50$ rad/s, $J_{mn} = 0.1$ kg-m^2, $K_{tn} = 5$ N-m/A have been taken. The fig. (5.4) represents the applied and estimated disturbance.

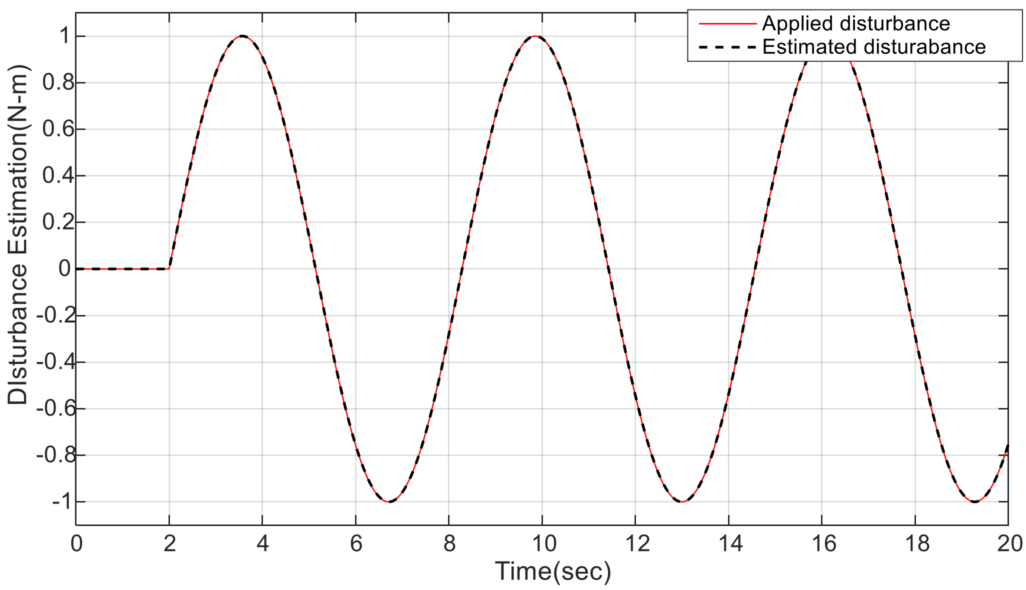

Fig. 5.4- Reference angle tracking when sinusoidal angle reference and sinusoidal disturbance is applied at t=0, t=2 sec respectively

5.3 Proposed PID Controller and DOB based Position Control System:

5.3.1 Brief overview of PID Controller tuning:

In this section we will first design PID Controller then we will use it with the DOB based system. It is well known fact that PID is most popular control method due to its simplicity and effective performance. Till date so many PID tuning methods have been proposed [27], but none of them meets the desired performance in motion control. The most common tuning method was proposed by Ziegler-Nichols but this methods big overshoot, robustness to time varying parameter is low, and it also needs many iterations. There is also one method Cohen-Coon formula [28]-[[29] which was invented for better robustness but it gives big overshoot and oscillatory response. There are also advanced methods such as Rivera's method [ref to 10] and many intelligent tuning methods like Genetic algorithm (GA), Fruit fly optimization [28],[29]. Though this advanced methods are superior than the conventional ones but the main problem with these methods are that they are too complex to use. Main problem of these tuning methods for motion control is its complex system dynamics, uncertainties, unknown disturbances etc. To handle this problem a practical PID tuning method [30] has been used in this thesis. It uses the advantage of 2-DOF approach. It provides high robustness to unmodelled dynamics, uncertainties etc.

5.3.2 PID Controller tuning:

Here a parallel form PID controller is tuned for position control system. The BD is shown below

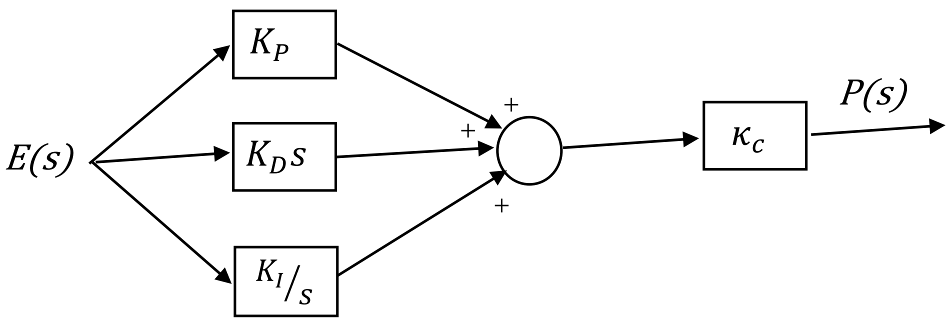

Fig. 5.5- Parallel form PID [27]

Here the assumption is that servo system is free from external disturbances and it is linear. One more assumption is that the system inertia should be chosen to the upper bound of exact inertia. So, the desired gains according to desired natural frequency and damping co-efficient

$$K_P^{des} = J_{mn}\omega_n^2$$

$$K_D^{des} = J_{mn} 2\zeta\omega_n$$

Now, the real controller gains

$$K_P = J_{mn}\omega_n^2 + K_D^{des} R$$

$$K_I = K_D^{des} R$$

$$K_D = K_D^{des}$$

Where, R is the robustness variable. Higher the value of R higher will be the robustness until the system gets affected negatively due to practical constraint like noise.

From the previous section, i.e. in robustness analysis we get the values of $\zeta\omega_n, \omega_n^2$.

$2\zeta\omega_n = g_v$ and $\omega_n = \sqrt{\alpha\kappa} g_{dob}$ from eq (5.3) respectively.

Putting R as $g_{dob} = 50$ rad/s, $g_v = 100$ rad/s we get

$K_P = 1000$, $K_I = 500$, $K_D = 10$.

5.3.3 Position Control System analysis with PID Controller & DOB:

The BD is shown below

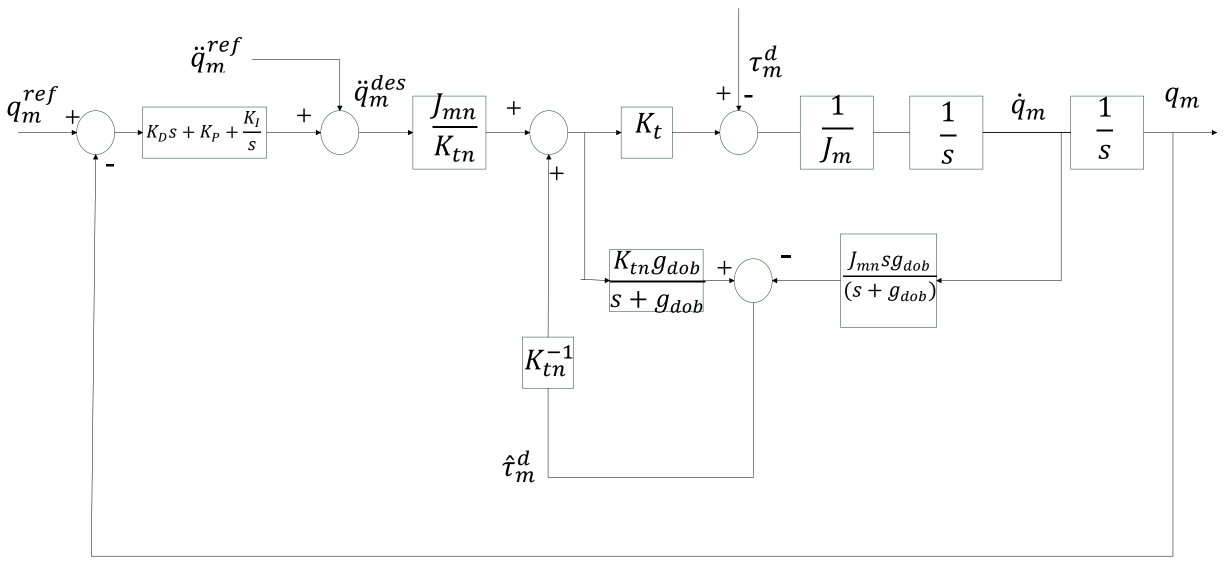

Fig. 5.6- Proposed PID controller & Dob based position control system

q_m^{ref} and $\ddot{q}_m^{ref}$ denotes angle/position and acceleration reference inputs respectively. A PID controller is used to achieve performance goals. The transfer function between $\ddot{q}_m^{ref}$ and q_m^{ref} derived from fig. (5.6) can be written as

$$\frac{\ddot{q}_m}{\ddot{q}_m^{ref}} = \frac{\alpha s^3 (s + g_{dob})}{s^3 (s + \alpha g_{dob}) + \alpha (s + g_{dob})(K_D s^2 + K_P s + K_I)} \tag{5.6}$$

When g_v is infinite. And,

$$\frac{\ddot{q}_m}{\ddot{q}_m^{ref}} = \frac{\alpha s^3 (s + g_v)(s + g_{dob})}{s^3 (s^2 + g_v s + \alpha g_v g_{dob}) + \alpha (s + g_v)(s + g_{dob})(K_D s^2 + K_P s + K_I)} \tag{5.7}$$

When g_v is finite.

5.3.4 Transfer function derivation:

Case 1: When g_v is infinite:

From equation (5.1) it is found that

$$\frac{\ddot{q}_m}{\ddot{q}_m^{des}} = \alpha \left(\frac{s + g_{dob}}{s + \alpha g_{dob}} \right) \tag{5.8}$$

The simplified BD of fig. (5.6) has shown below

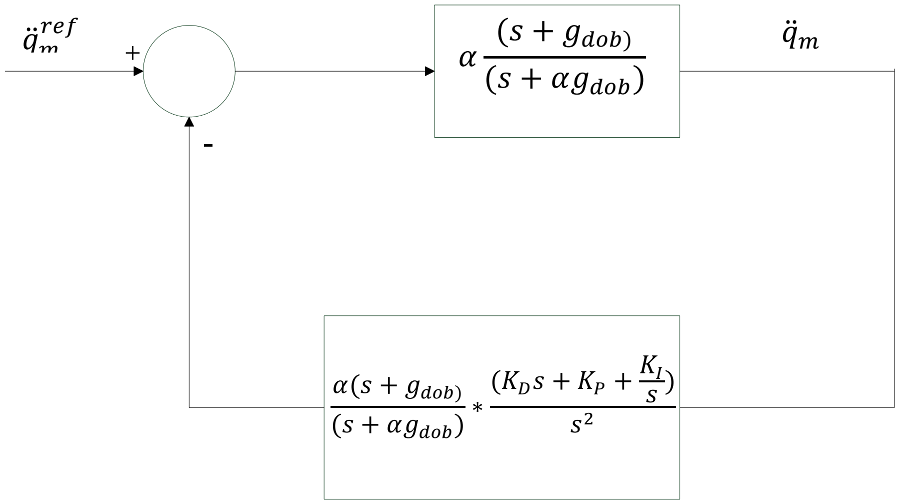

Fig. 5.7- Simplified block diagram of fig. (5.6)

$$\frac{\ddot{q}_m}{\ddot{q}_m^{ref}} = \frac{\alpha\left(\frac{s+g_{dob}}{s+\alpha g_{dob}}\right)}{1+\alpha\left(\frac{s+g_{dob}}{s+\alpha g_{dob}}\right)\left(\frac{(K_D s^2+K_P s+K_I)}{s^3}\right)}$$

$$\frac{\ddot{q}_m}{\ddot{q}_m^{ref}} = \frac{\alpha s^3(s+g_{dob})}{s^3(s+\alpha g_{dob})+\alpha(s+g_{dob})(K_D s^2+K_P s+K_I)}$$

Case 2- when g_v is finite:

$$\frac{\ddot{q}_m}{\ddot{q}_m^{ref}} = \frac{\alpha\frac{(s+g_v)(s+g_{dob})}{s^2+g_v s+\alpha g_v g_{dob}}}{1+\alpha\frac{(s+g_v)(s+g_{dob})}{(s^2+g_v s+\alpha g_v g_{dob})}\left(\frac{(K_D s^2+K_P s+K_I)}{s^3}\right)}$$

$$\frac{\ddot{q}_m}{\ddot{q}_m^{ref}} = \frac{\alpha s^3(s+g_v)(s+g_{dob})}{s^3(s^2+g_v s+\alpha g_v g_{dob})+\alpha(s+g_v)(s+g_{dob})(K_D s^2+K_P s+K_I)}$$

It is obvious from the equations (5.6) and (5.7) that characteristic functions are dependent on $g_{dob}, g_v, \alpha\ \ K_P, K_D$.

5.3.5 Stability analysis:

Let us consider the equation () by using RH criterion to perform stability analysis we get

$$\alpha^{-1} < \frac{(K_D + g_{dob})(K_P + g_{dob}K_D)}{K_I + g_{dob}K_P}$$

This above equation is the stability criteria. From this equation it can be concluded that stability of robust position control can be improved by increasing the value of α and g_{dob}. But from the robustness analysis i.e. from equation (5.5) it has been observed that α and g_{dob} can not be freely increased. This is the trade-off between robustness and stability.

Generally it is assumed that robustness and performance can be controlled in inner and outer loop separately, but it is not true indeed. The robustness depends on outer loop as well. It will be clarified by deriving T_{PC}^{SEN} and T_{PC}^{CoSEN}.

$$T_{PC}^{SEN} = \frac{1}{1 + L_{PC}(s)}$$

$$T_{PC}^{CoSEN} = \frac{L_{PC}(s)}{1 + L_{PC}(s)}$$

$$L_{PC}(s) = \alpha \frac{g_{dob}s^3 + (s + g_{dob})(K_D s^2 + K_P s + K_I)}{s^4} \quad (5.9)$$

When g_v is infinite, and

$$L_{PC}(s) = \alpha \frac{g_{dob}g_v s^3 + (s + g_{dob})(s + g_v)(K_D s^2 + K_P s + K_I)}{s^4(s + g_v)} \quad (5.10)$$

When g_v is finite.

From equation of T_{PC}^{SEN} , T_{PC}^{CoSEN} it is observed that increasing the outer loop controller gain leads to more robust system when $\alpha g_{dob} > 0.5 g_v$ .Still, inner loop becomes sensitive to high frequency noises. Again, increasing outer loop controller gain has several disadvantages like energy consumption, vibration due to high frequency dynamics etc.

Derivation of $L_{PC}(s)$:

Case1- when g_v is infinite:

The characteristic equation from (5.6) we get

$$C_h(s) = s^3(s + \alpha g_{dob}) + \alpha(s + g_{dob})(K_D s^2 + K_P s + K_I)$$

By rearranging we get

$$C_h(s) = s^4 + \alpha[g_{dob}s^3 + (s + g_{dob})(K_D s^2 + K_P s + K_I)]$$

$$s^4[1 + \frac{\alpha\{g_{dob}s^3 + (s + g_{dob})(K_D s^2 + K_P s + K_I)\}}{s^4}$$

So, loop transfer function

$$L_{PC}(s) = \frac{\alpha[g_{dob}s^3 + (s + g_{dob})(K_D s^2 + K_P s + K_I)]}{s^4}$$

Case2- when g_v is finite:

The characteristic equation from () we get

$$C_h(s) = s^3(s^2 + g_v s + \alpha g_v g_{dob}) + \alpha(s + g_v)(s + g_{dob})(K_D s^2 + K_P s + K_I)$$

By rearranging we get

$$C_h(s) = s^4(s + g_v) + \alpha[g_v g_{dob}s^3 + (s + g_v)(s + g_{dob})(K_D s^2 + K_P s + K_I)]$$

$$s^4(s + g_v)[1 + \frac{\alpha\{g_v g_{dob}s^3 + (s + g_v)(s + g_{dob})(K_D s^2 + K_P s + K_I)\}}{s^4(s + g_v)}$$

So, loop transfer function

$$L_{PC}(s) = \frac{\alpha[g_v g_{dob}s^3 + (s + g_v)(s + g_{dob})(K_D s^2 + K_P s + K_I)]}{s^4(s + g_v)}$$

5.4 Simulations:

The following bode magnitude plots for Co-sensitivity functions have been done taking different values of α and using the value of the parameters as- $g_{dob} = 50$ rad/s, $g_v = 100$ rad/s, $K_P = 1000$, $K_I = 500$, $K_D = 10$.

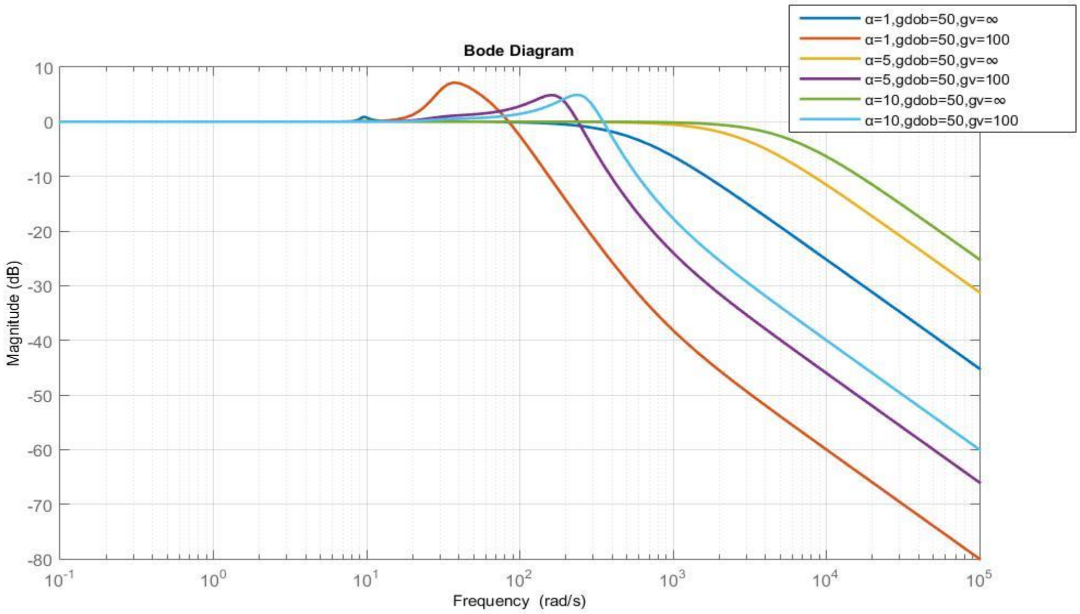

Fig.5.8- Co-sensitivity function frequency response for outer-loop

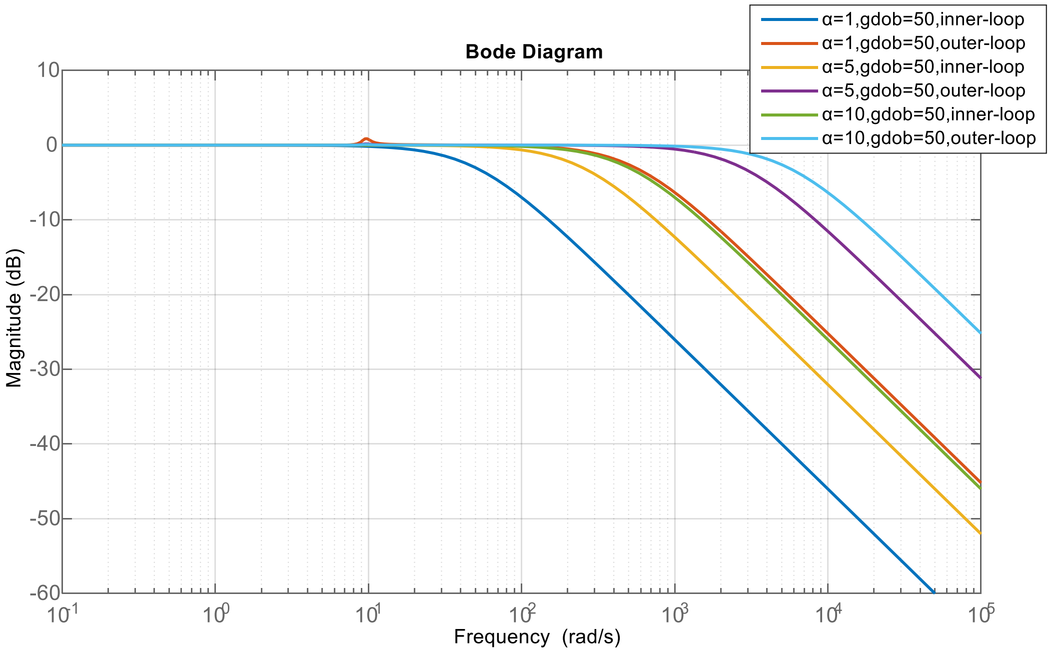

Fig.5.9- Co-sensitivity function frequency response for inner-loop and outer-loop

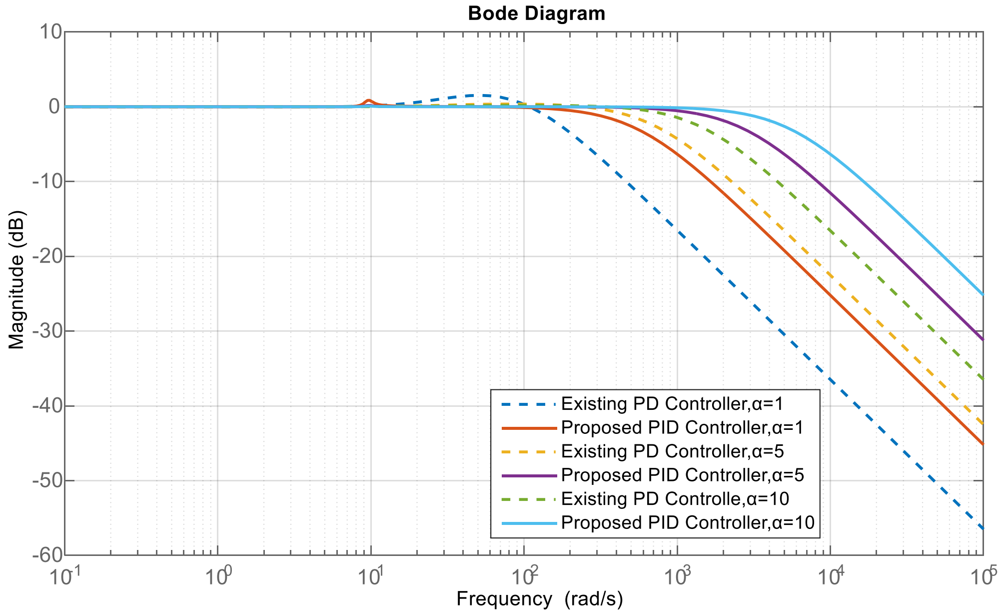

Fig.5.10- Comparison of Co-sensitivity function frequency response for outer-loop

From fig. (5.8) it can be seen that bandwidth for ideal velocity estimation is higher than the practical one for every values of α. Again, it is observed from fig. (5.9) that using the PID controller in outer-loop increases the bandwidth along with robustness. Fig. (5.10) shows a comparative plot for outer-loop Co-sensitivity function between existing PD controller & DOB and proposed PID controller & DOB. For proposed controller the bandwidth is higher which means more robustness.

Now, the root locus diagram has been shown below for stability analysis

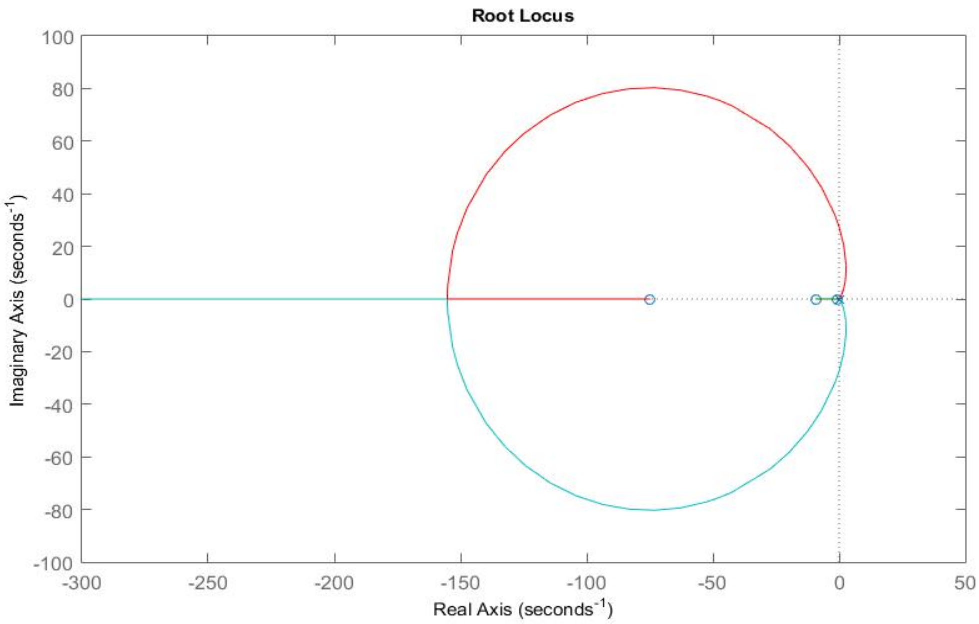

Fig. 5.11- Root locus plot for stability analysis

Similar to the root locus plot in chapter 4 this figure also clearly describes that on increasing the α, i.e. the gain value, the plot is shifting towards left, thereby increasing stability. Though the increment is limited by robustness constraint as described earlier.

The position tracking response is shown below when sinusoidal angle reference and sinusoidal disturbance of magnitude one is applied at t=0, t=2 sec respectively.

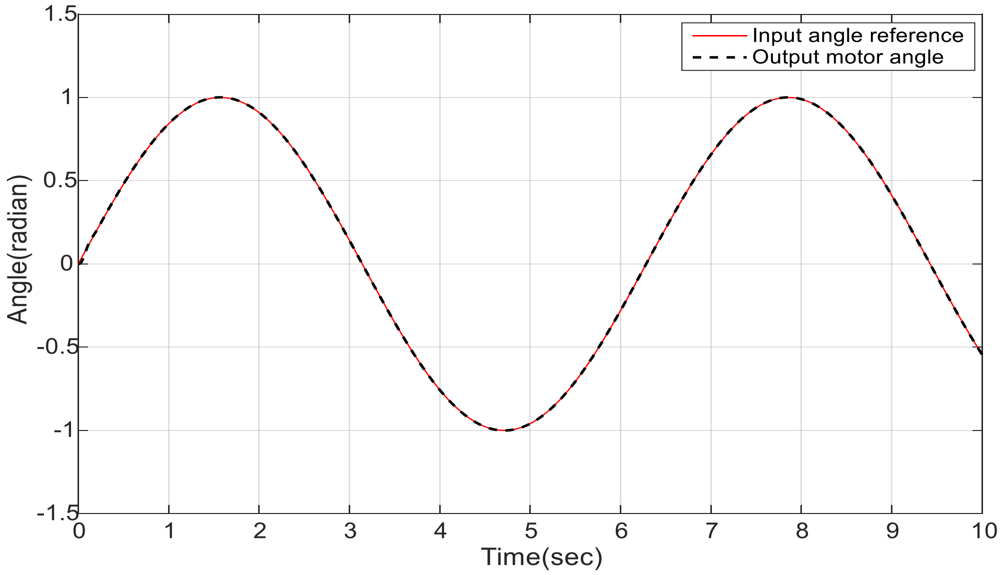

Fig.5.12- Position Control response when sinusoidal input is applied at t=0 and sinusoidal disturbance at t=2 sec

It can be clearly stated that reference angle tracking is done very precisely. Position tracking error has been shown with different inputs in chapter 6.

Chapter 6

COMPARISON OF PERFORMANCE

6.1 Introduction:

In this chapter, disturbance estimation error and tracking error plots have been shown between existing PD controller & DOB based position control system [24] and proposed PID Controller & DOB based position control system. Simulations have been done using different waveforms applied at different time such that the effects of those waveforms can be clearly observed on outputs be it estimated disturbance or motor output angle. The error plots are then followed by observations.

The following waveforms have been used as inputs

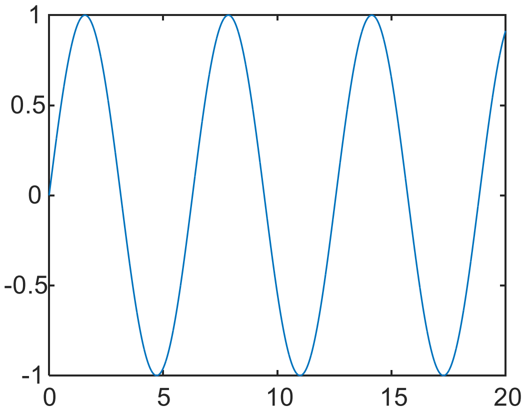

Fig. 6.1a

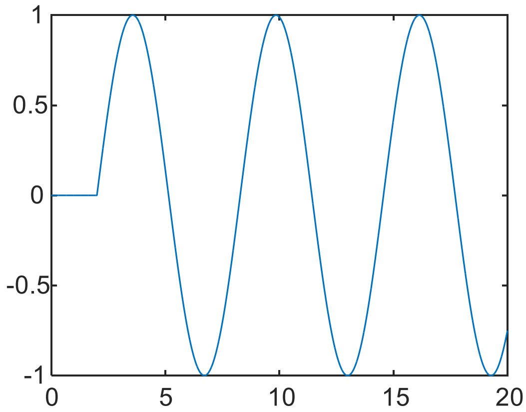

Fig. 6.1a

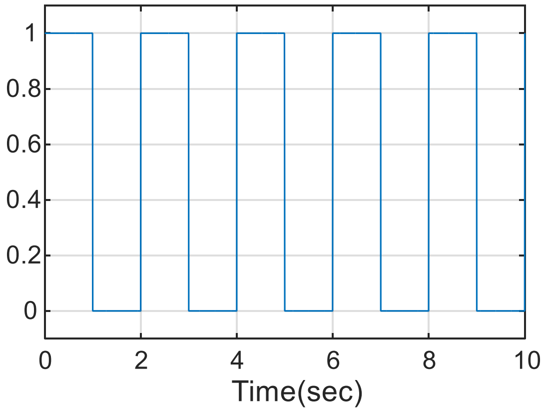

Fig. 6.1c

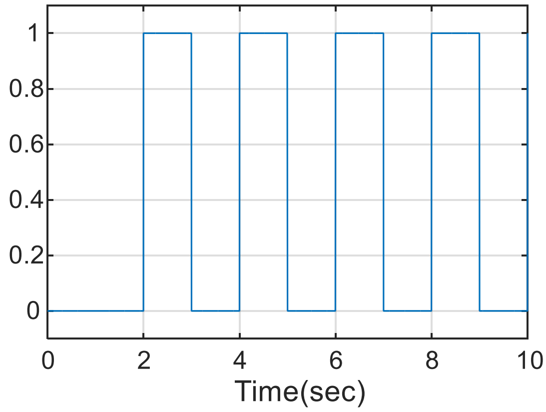

Fig. 6.1d

Fig. 6.1- Different type of input waveforms used as position reference or disturbance, (a), (b)- sinusoidal input applied at t=0 and t=2 respectively; (c), (d)- square input applied at t=0 and t=2 respectively

6.2 Disturbance estimation error:

6.2.1 Plots for ideal velocity measurement considering only external disturbances and parameter uncertainties to be zero:

In this section the plots have been shown for ideal velocity estimation case, i.e. when $g_{dob} =$ 50 rad/s, g_v is infinite.

Case 1:

Fig.(6.1a) and Fig.(6.1b) has been applied as position reference and disturbance respectively.

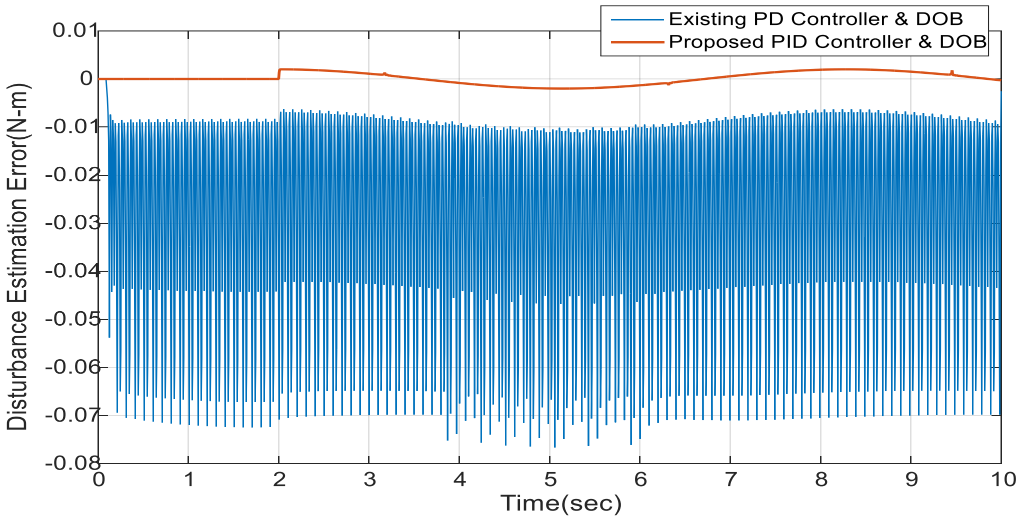

Fig.6.2- Disturbance estimation error when sinusoidal input as position reference and sinusoidal disturbance is applied at t=0 and t=2 sec respectively

Observation:

Up to 2 seconds error is zero for proposed one whereas error is non-zero. At t=2 sec, there are transients in both the plots. The value of error is less for proposed controller & DOB.

Case 2:

In this test case fig.(6.1c) and fig.(6.1b) has been applied as position reference and disturbance respectively.

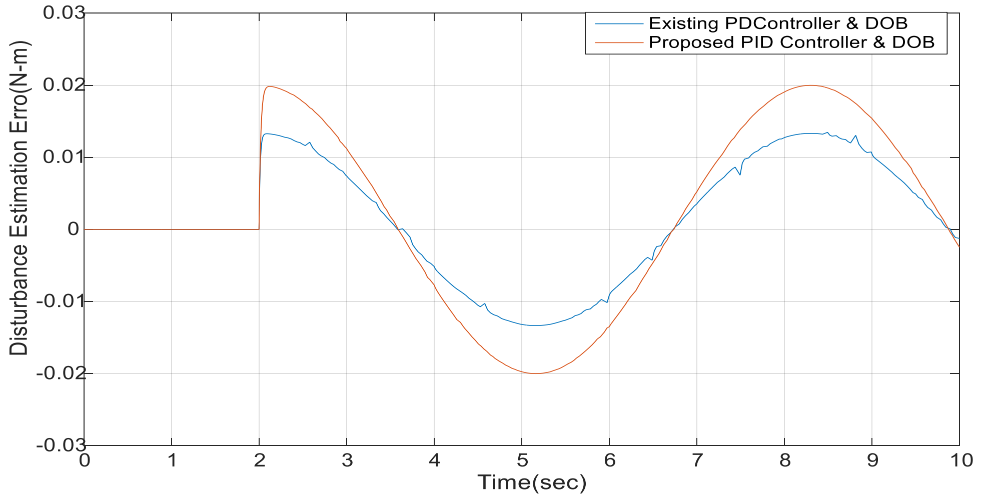

Fig.6.3- Disturbance estimation error when square input as position reference and sinusoidal disturbance is applied at t=0 and t=2 sec respectively

Observation:

Both the plots are slightly phase delayed, but the magnitude is less in case of existing PD controller & DOB. But there are some spikes of very little magnitude in case of existing PD controller & DOB, whereas for the proposed PID controller & DOB the plot is smoother.

Case 3:

In this test case fig.(6.1a) and fig.(6.1d) has been applied as position reference and disturbance respectively.

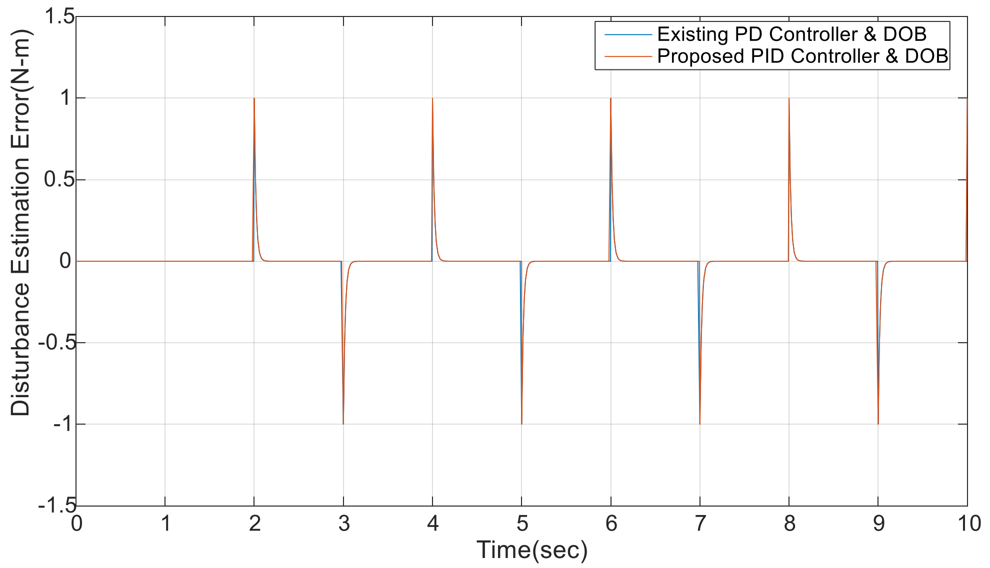

Fig.6.4a- Disturbance estimation error when sinusoidal input as position reference and square disturbance is applied at t=0 and t=2 sec respectively

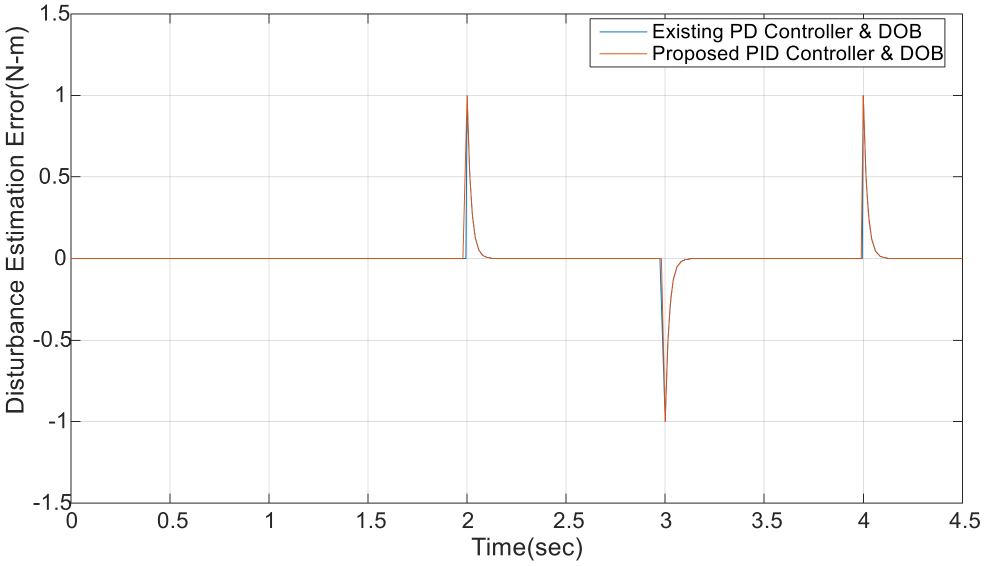

Fig.6.4b- Disturbance estimation error when sinusoidal input as position reference and square disturbance is applied at t=0 and t=2 sec respectively (zoomed up to 4.5 seconds)

Observation:

There are impulses of magnitude one at the positive and negative edge of the applied disturbance. This is caused by delay provided from low pass filter. Proposed method is providing slightly faster response.

Case 4:

In this test case fig.(6.1c) and fig.(6.1d) has been applied as position reference and disturbance respectively.

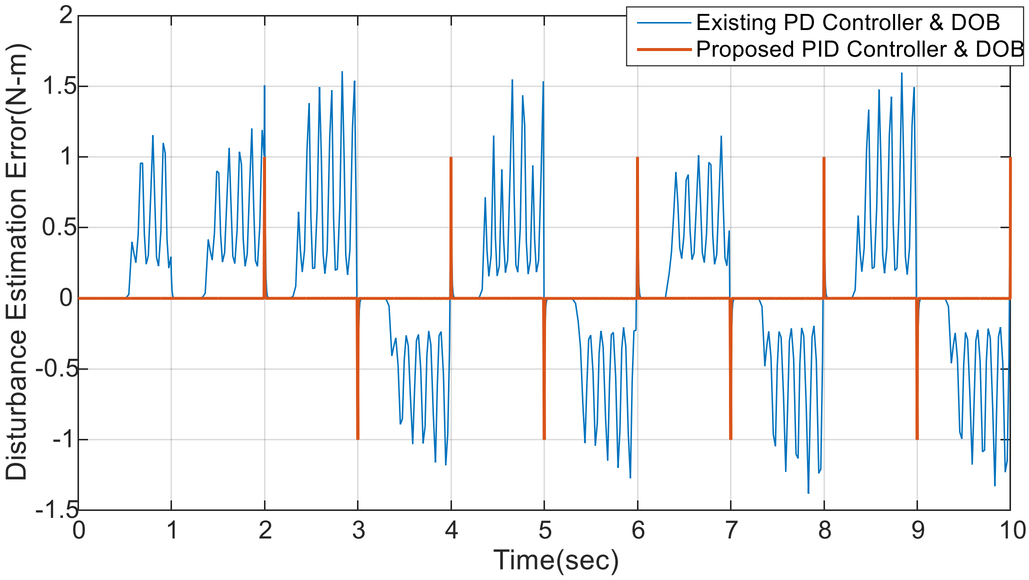

Fig.6.5- Disturbance estimation error when square input as position reference and square disturbance is applied at t=0 and t=2 sec respectively

Observation:

Sharp impulses can be observed at the edges of applied disturbance. Rest of time error is zero. But the existing PD controller & DOB is not measuring the disturbance in this case.

6.2.2 Plots for practical velocity measurement considering only external disturbances and parameter uncertainties to be zero:

Now the plots have been shown for practical velocity estimation case, i.e. when $g_{dob} = 50$ rad/s, $g_v = 100$ rad/s.

Case 1:

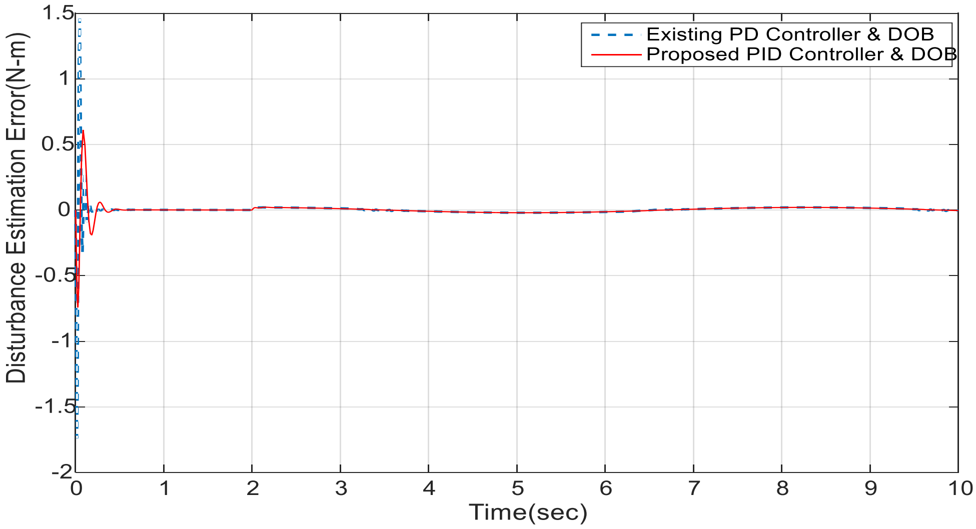

Fig.6.6- Disturbance Estimation Error of the system for sinusoidal input and sinusoidal disturbance applied at t=0 and t=2 respectively

Observation:

Transients are present at start, then it decays to zero quickly. The magnitude is higher for existing PD controller & DOB.

Case 2:

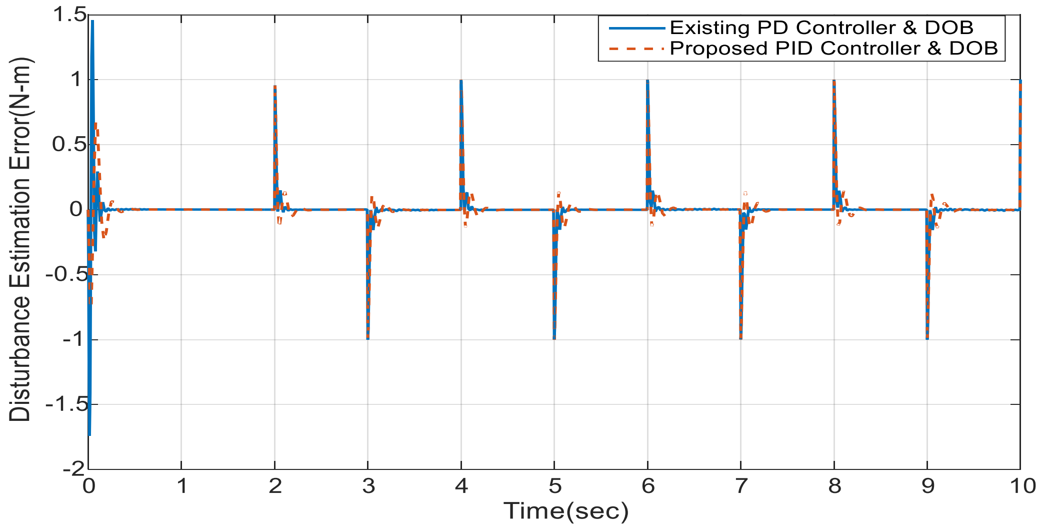

Fig.6.7a- Disturbance Estimation Error of the system for sinusoidal input and square disturbance applied at t=0 and t=2 respectively

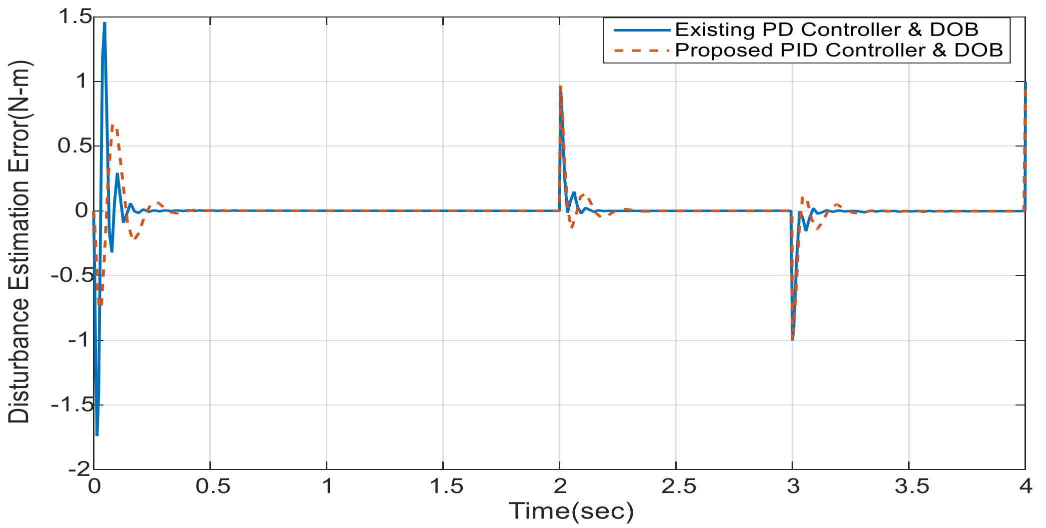

Fig.6.7b- Disturbance Estimation Error of the system for sinusoidal input and square disturbance applied at t=0 and t=2 respectively (zoomed up to 4sec)

Observation:

Transients are present at start, then it decays to zero quickly. The magnitude is higher for existing PD controller & DOB. Impulses are present at the edges of applied disturbance. The transients decays to zero slightly slower in case of proposed PID controller & DOB.

6.2.3 Plots for ideal velocity measurement considering external disturbances and parameter uncertainties:

Torque co-efficient(k_t) is taken as 5.01, inertia co-efficient(J) is taken as 0.095.

Case 1:

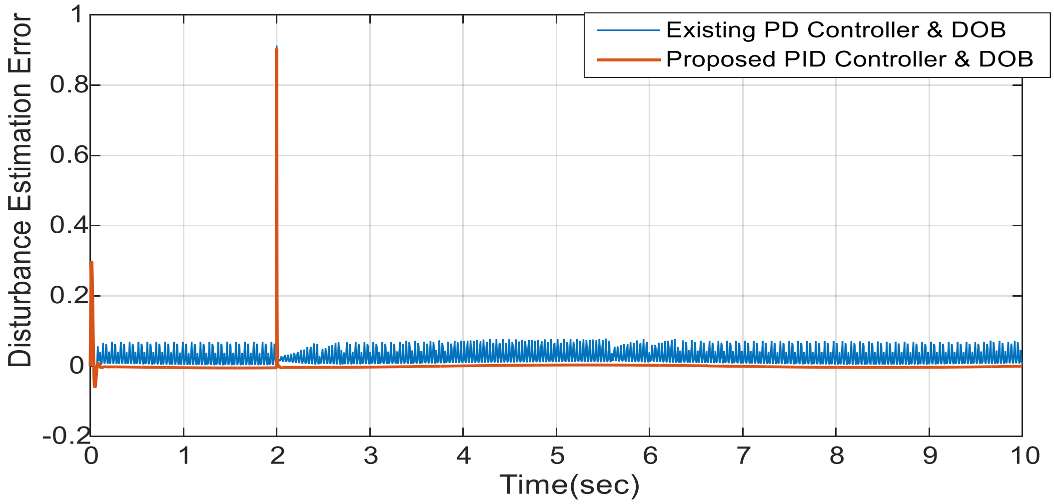

Fig.6.8-Disturbance Estimation Error of the system for sinusoidal input and sinusoidal disturbance applied at t=0 and t=2 respectively

Observation:

Disturbance Estimation Error is zero except at t=0 for proposed PID Controller & DOB, a transient is also observed at t=2 sec due to the application of disturbance at the same time; whereas for the existing PD Controller & DOB non zero error exists.

Case 2:

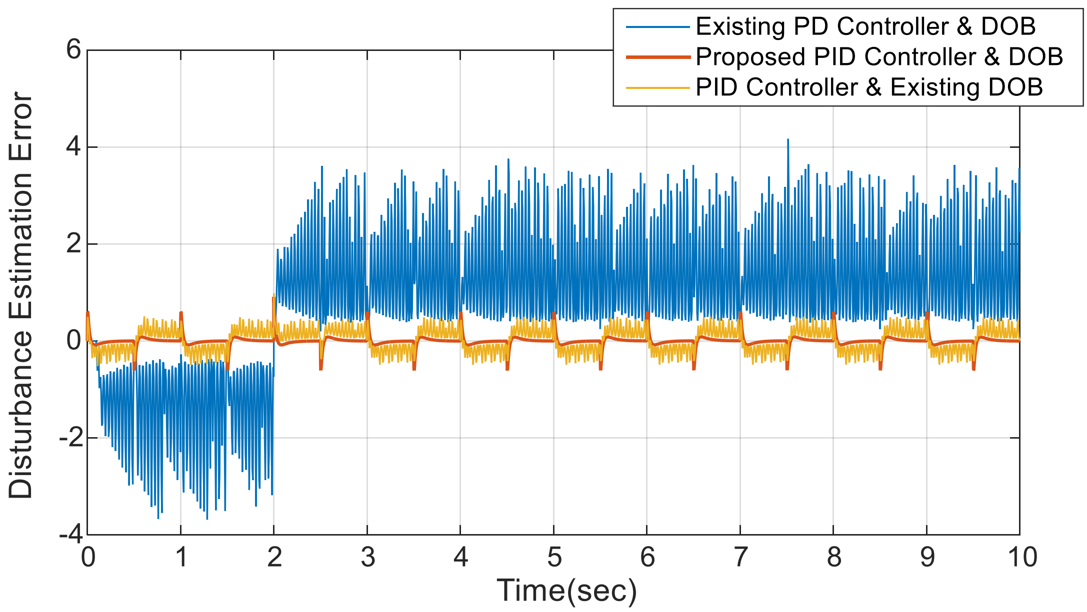

Fig.6.9a-Disturbance Estimation Error of the system for square input and sinusoidal disturbance applied at t=0 and t=2 respectively

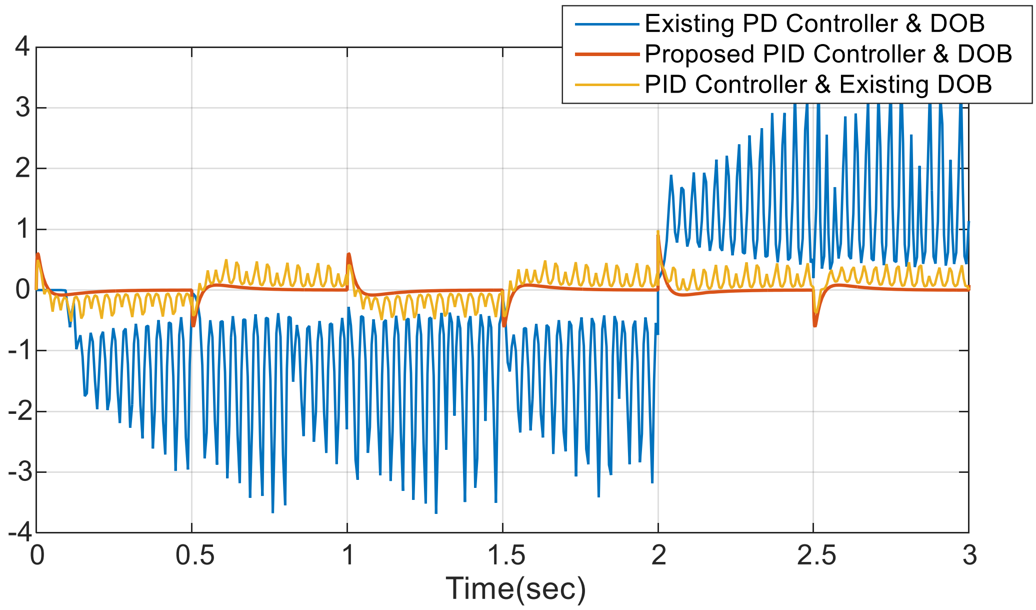

Fig.6.9b-Disturbance Estimation Error of the system for square input and sinusoidal disturbance applied at t=0 and t=2 respectively (zoomed up to 3sec)

Observation:

Disturbance Estimation Error is zero except at the edges of input waveform for proposed PID controller & DOB. At t=2 sec, transients are seen in the figure (6.9b) due to the disturbance applied on the same time. This is much better than existing one.

Case 3:

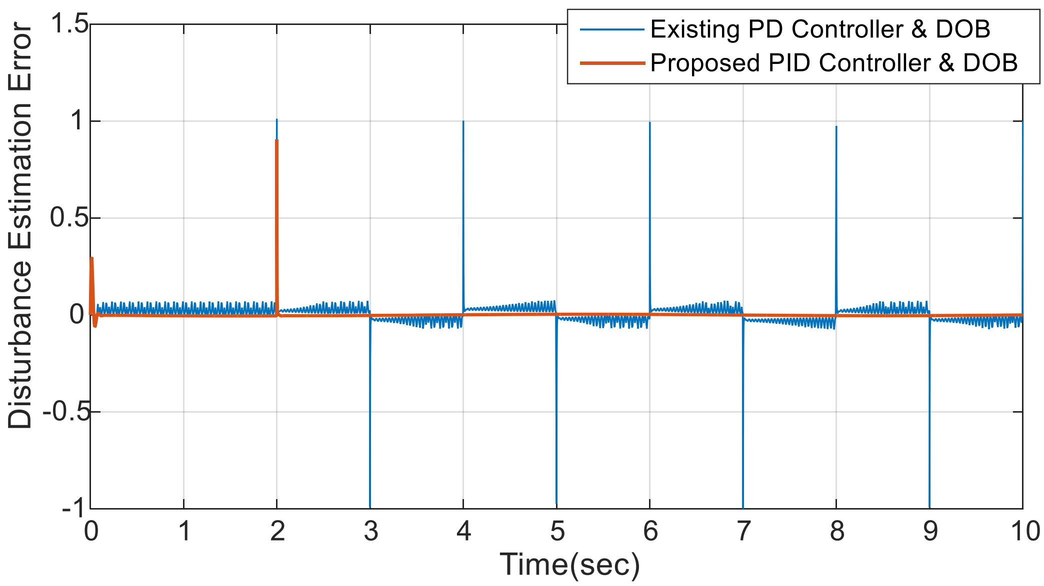

Fig.6.10- Disturbance Estimation Error of the system for sinusoidal input and square disturbance applied at t=0 and t=2 respectively

Observation:

Disturbance Estimation Error is zero except at the sharp edges of the applied disturbance. Proposed PID controller & DOB shows better disturbance estimation.

Case 4:

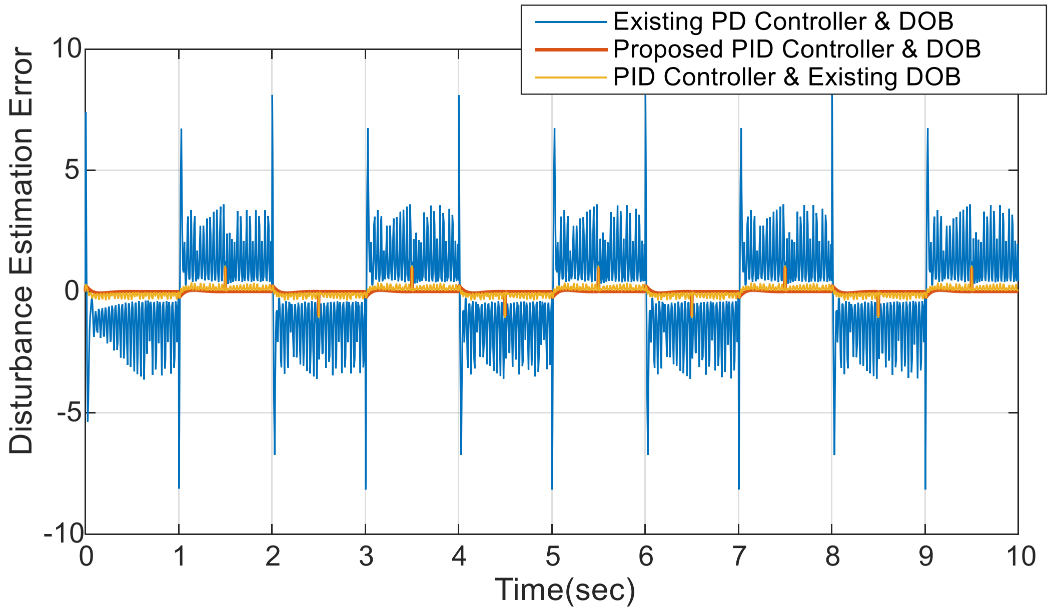

Fig.6.11a- Disturbance Estimation Error of the system for square input and square disturbance applied at t=0 and t=1.5 respectively

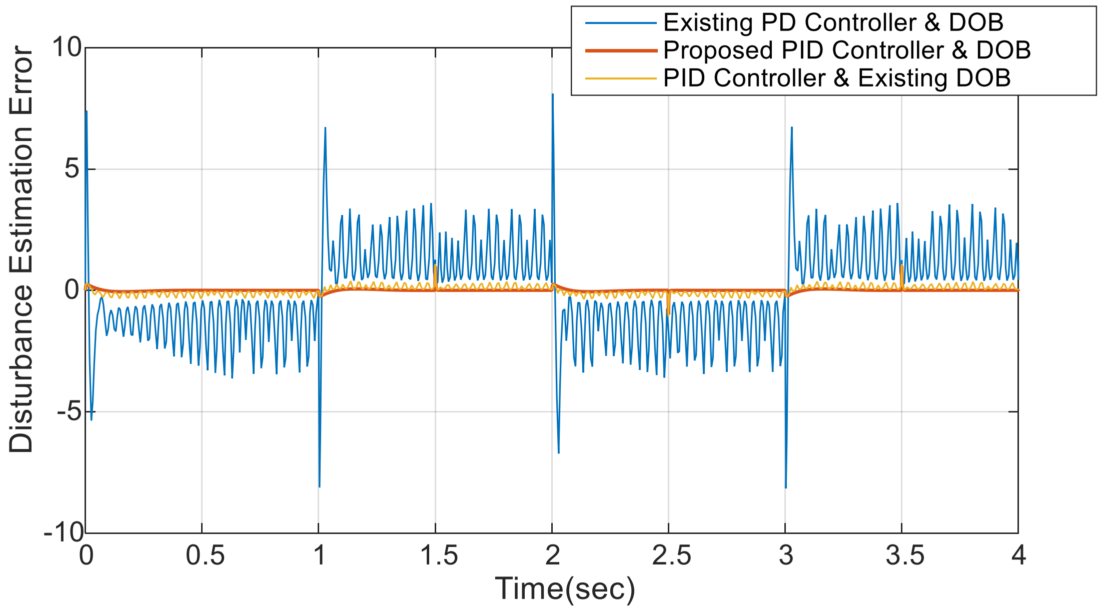

Fig.6.11b- Disturbance Estimation Error of the system for square input and square disturbance applied at t=0 and t=1.5 respectively (zoomed up to 4 seconds)

Observation:

Disturbance estimation is done much better by proposed PID controller & DOB. Impulses are present for proposed PID controller & DOB and PID controller & existing DOB. Disturbance estimation is very poorly done in case of proposed PD controller & DOB.

6.3 Tracking error:

6.3.1 Tracking error plots considering ideal velocity measurement in presence of external disturbances and parameter uncertainties to be zero:

Case 1:

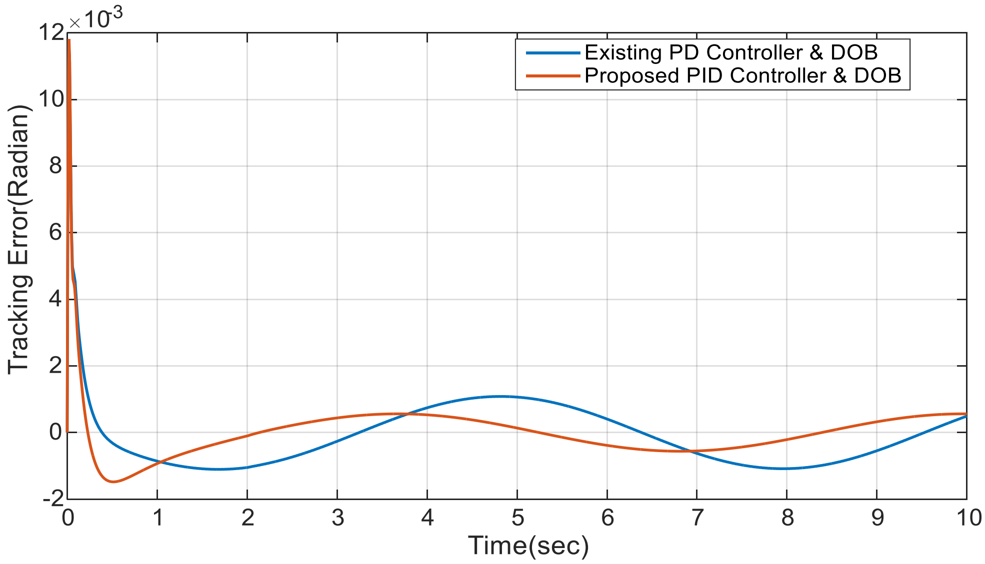

Fig.6.12- Tracking error when sinusoidal input as position reference and sinusoidal disturbance is applied at t=0 and t=2 sec respectively

Observation:

The magnitude of error for both plots is very less. Both the graphs have slight phase difference with the input reference.

Case 2:

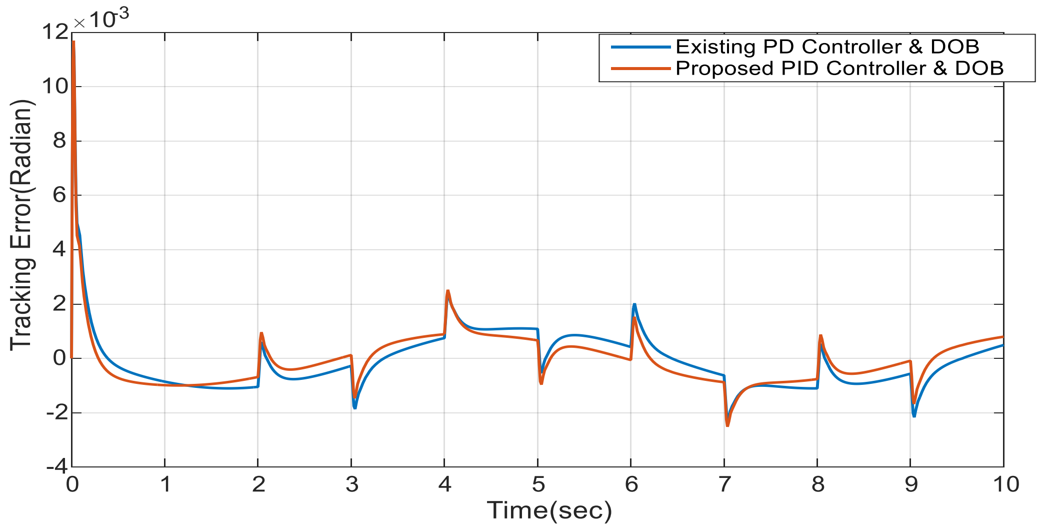

Fig.6.13- Tracking error when sinusoidal input as position reference and square disturbance is applied at t=0 and t=2 sec respectively

Observation:

Transient of little magnitude is observed at edges of applied disturbance from the above figure. The error value is almost same.

Case 3:

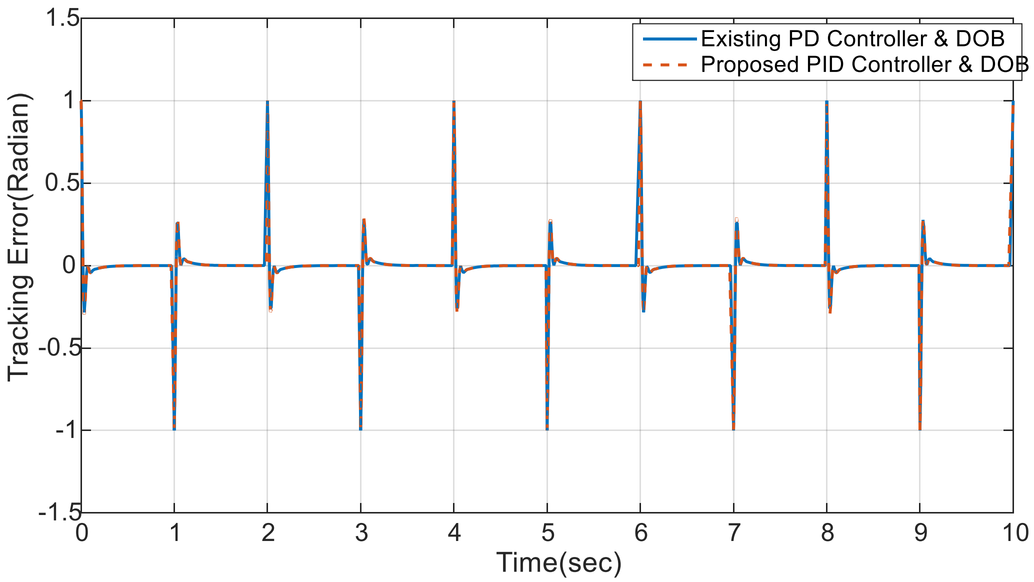

Fig.6.14a- Tracking error when square input as position reference and sinusoidal disturbance is applied at t=0 and t=2 sec respectively

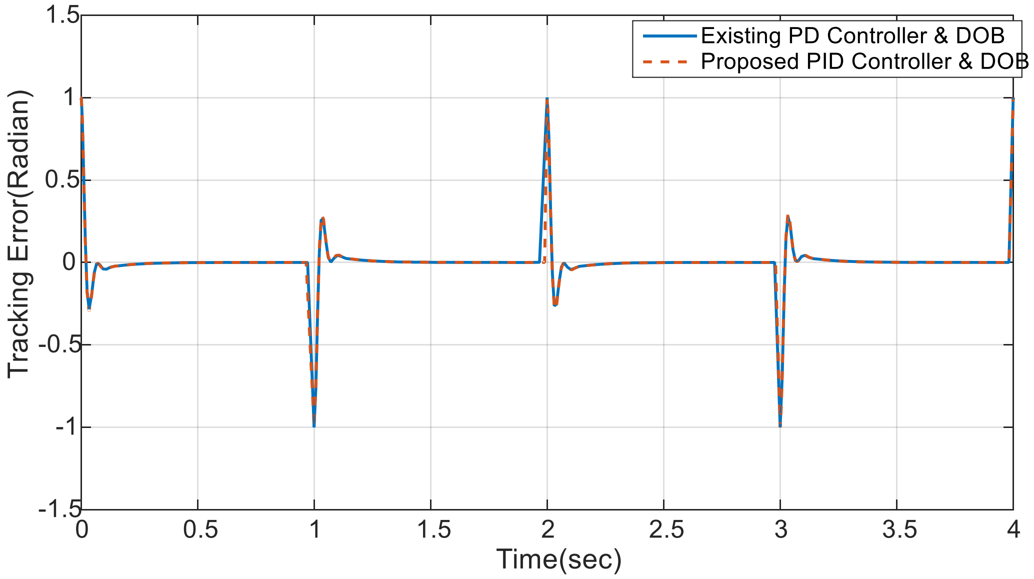

Fig.6.14b- Tracking error when square input as position reference and sinusoidal disturbance is applied at t=0 and t=2 sec respectively (zoomed up to 4 seconds)

Observation:

There are transients at the edges of applied input angle reference. It decays to zero quickly. The error plots are same for both cases.

Case 4:

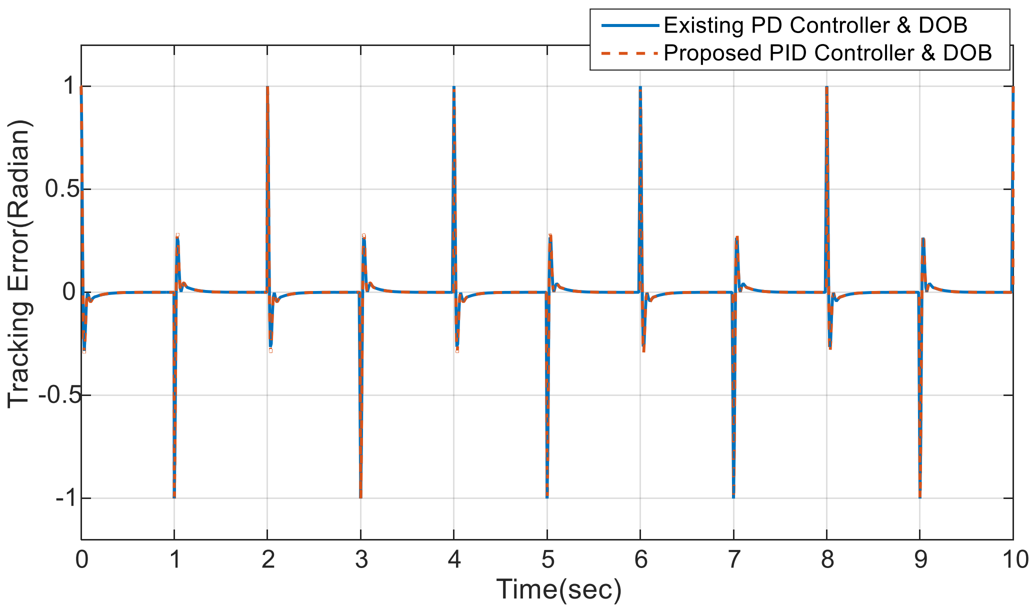

Fig.6.15a- Tracking error when square input as position reference and square disturbance is applied at t=0 and t=2 sec respectively

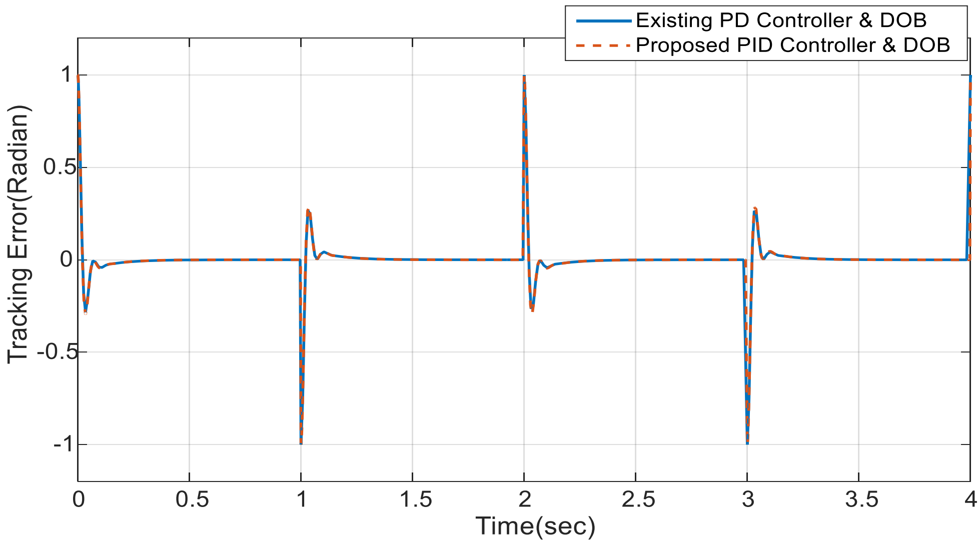

Fig.6.15b- Tracking error when square input as position reference and square disturbance is applied at t=0 and t=2 sec respectively (zoomed up to 4 seconds)

Observation:

Transients at the edges of applied input angle reference can be seen from the figure. It decays to zero quickly. The error plots are same for both cases.

6.3.2 Tracking error plots considering practical velocity measurement in presence of external disturbances and parameter variations are zero:

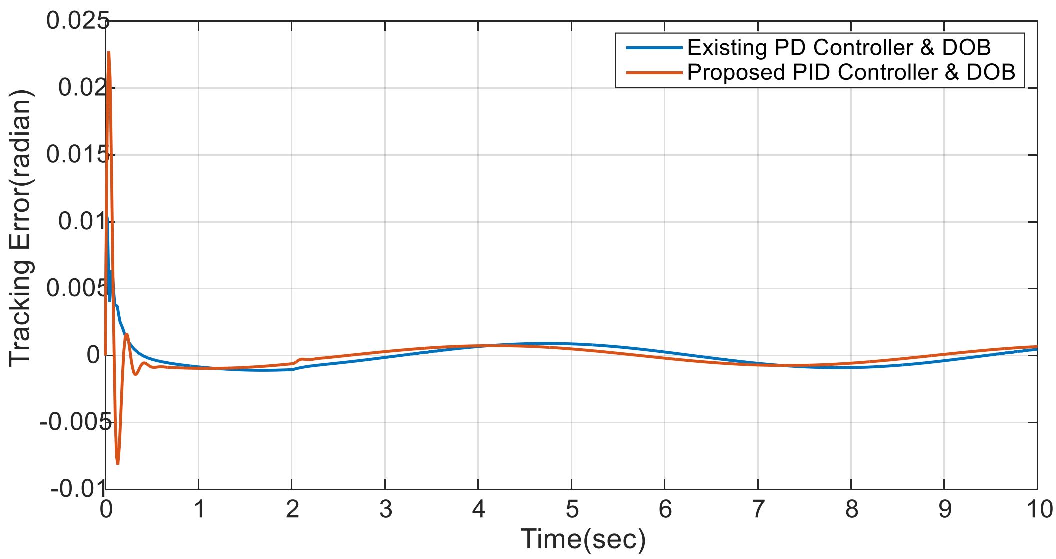

Fig.6.16- Tracking Error of the system for sinusoidal input and sinusoidal disturbance applied at t=0 and t=2 respectively

Observation:

Transients are present at start, the magnitude is higher for proposed one, but it rapidly decays to zero. At t=2 sec, a little fluctuation can be seen due to applied disturbance.

Case 4:

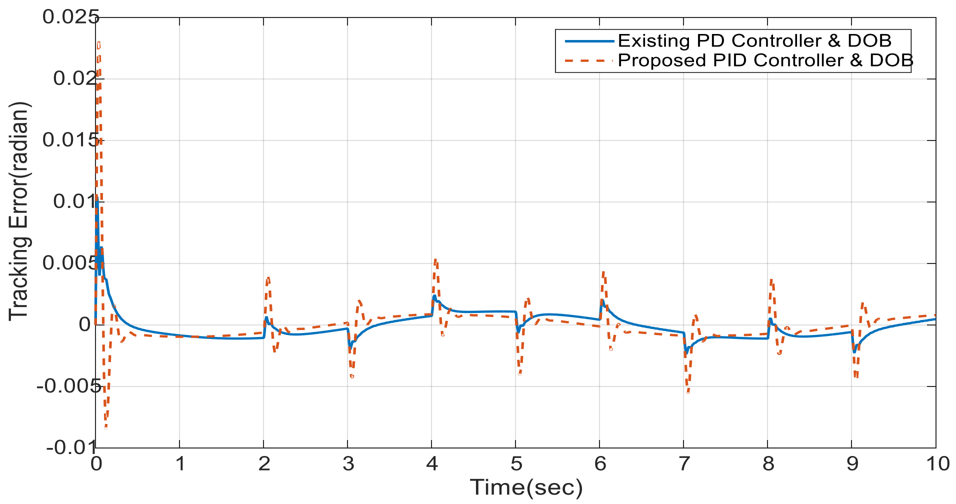

Fig.6.17-Tracking Error of the system for sinusoidal input and square disturbance applied at t=0 and t=2 respectively

Observation:

At start transient is present for both cases, then at sharp edges of the disturbance transients are again present. The value is higher for proposed PID controller & DOB.

6.3.3 Plots of tracking error for ideal velocity measurement considering external disturbances and parameter uncertainties:

Case 1:

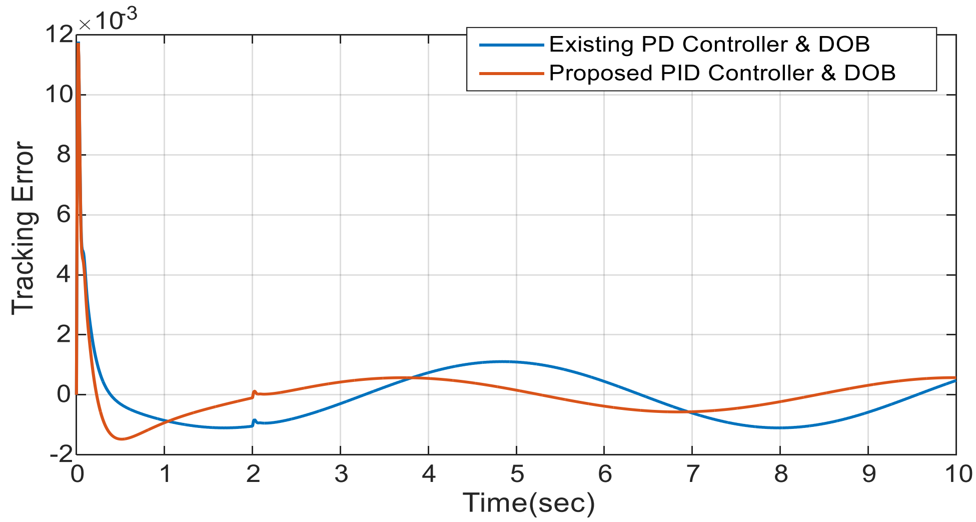

Fig.6.18- Tracking Error of the system for sinusoidal input and sinusoidal disturbance applied at t=0 and t=2 respectively

Observation:

Tracking error for the proposed PID Controller & DOB has been reduced slightly. Transients are observed at t=2sec, i.e. at the starting time of applied disturbance.

Case 2:

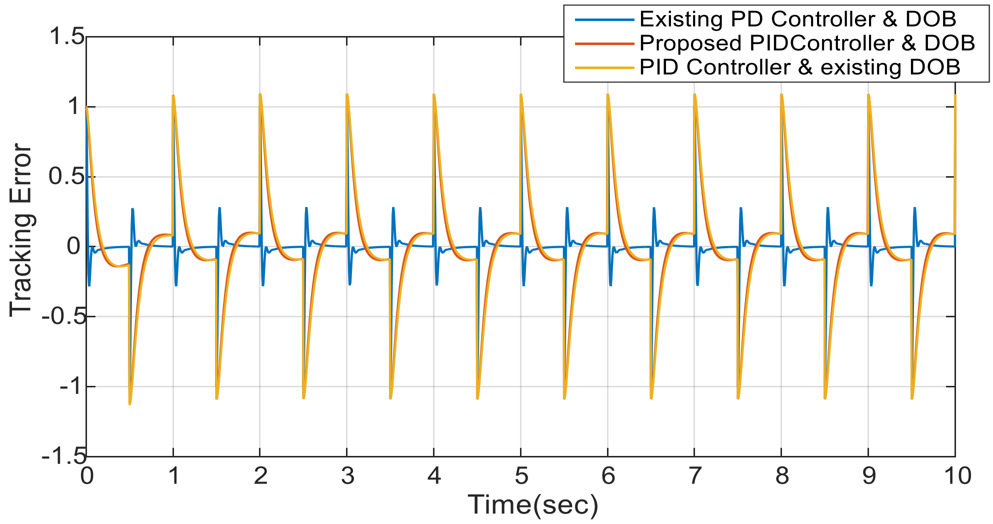

Fig.6.19a- Tracking Error of the system for square input and sinusoidal disturbance applied at t=0 and t=2 respectively

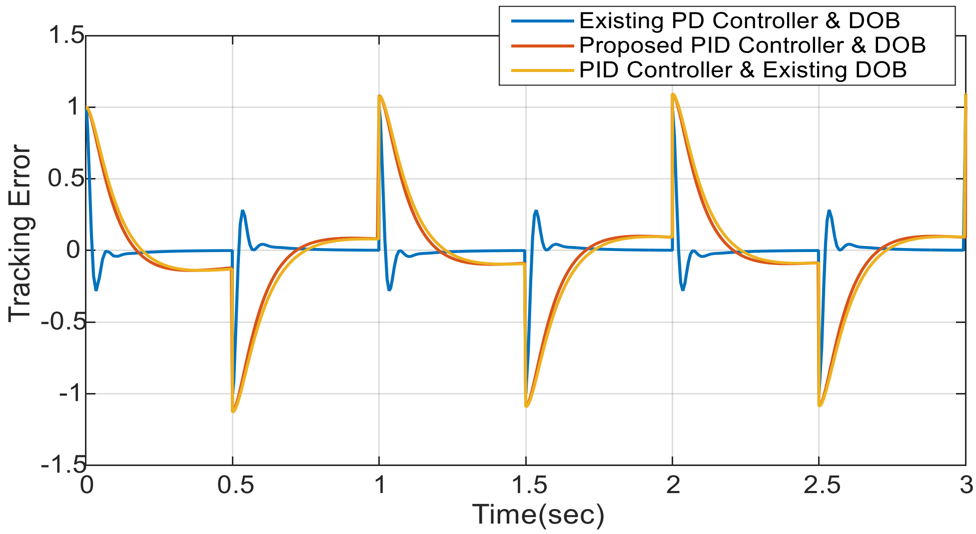

Fig.6.19b- Tracking Error of the system (zoomed up to 3 seconds) for square input and sinusoidal disturbance applied at t=0 and t=2 respectively

Observation:

Tracking error sluggishly decays to zero for proposed PID controller & DOB. For existing PD Controller & DOB error decays to zero quickly.

Case 3:

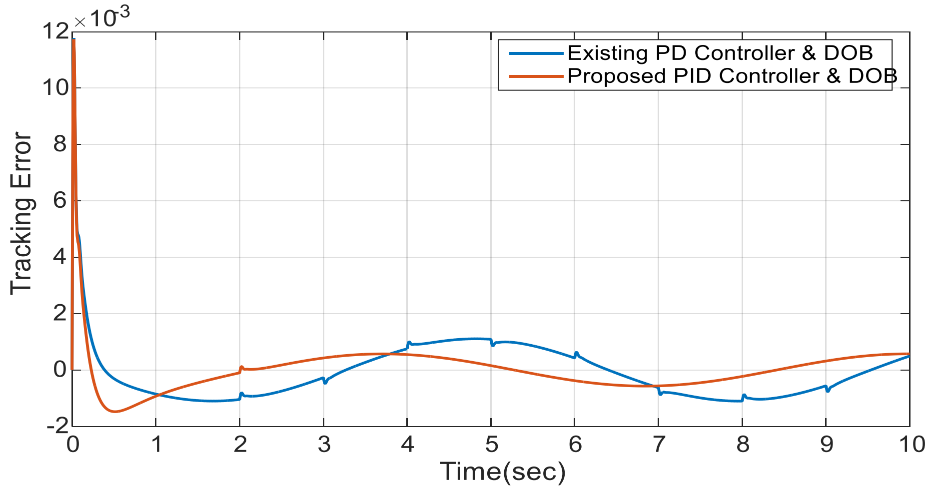

Fig.6.20- Tracking Error of the system for sinusoidal input and square disturbance applied at t=0 and t=2 respectively

Observation:

Tracking error for both the case are of very little magnitude having maximum value of $12*10^{-3}$ at t=0. Transients are present at the sharp edges of applied disturbance.

Case 4:

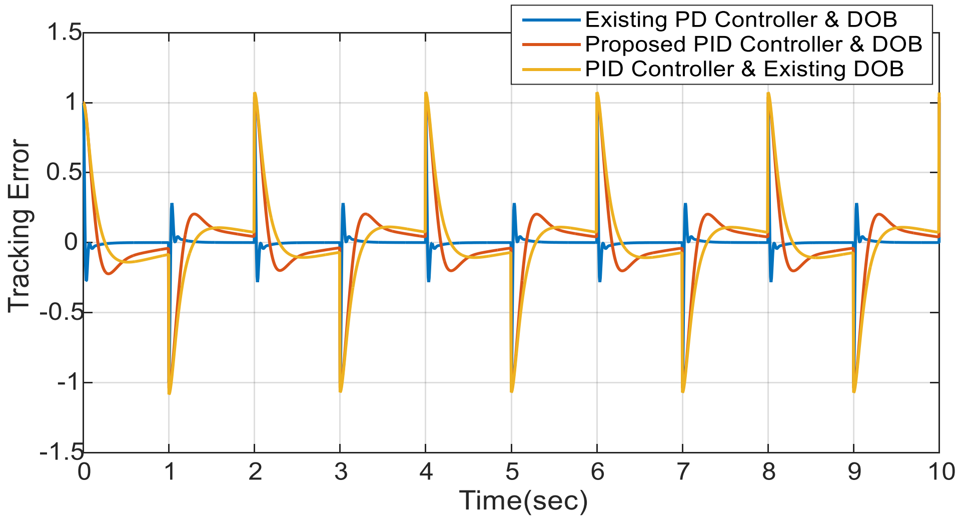

Fig.6.21a- Tracking Error of the system for square input and square disturbance applied at t=0 and t=1.5 respectively

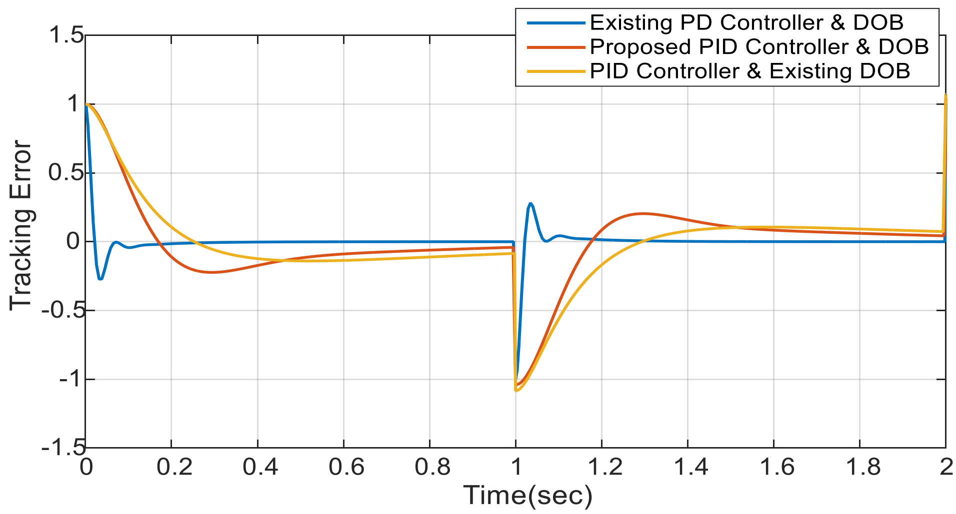

Fig.6.21b-Tracking Error of the system for square input and square disturbance applied at t=0 and t=1.5 respectively (zoomed up to 2 seconds)

Observation:

Tracking error decays to zero sluggishly for proposed PID controller & DOB, whereas the error quickly goes to zero for existing PD controller & DOB.

Chapter 7

Discussion and Conclusion

7.1 Discussion:

This section comprises of summary of each chapters except the introduction chapter. Chapter 2 is brief literature survey on applications of DOB, BW adjustment, new algorithm to make it more efficient tool. Chapter 3 describes the DOB design methods for minimum and non-minimum phase systems, why LPF is used along with examples to show the low pass filter design for the aforesaid systems can be done. Chapter 4 is the replication of the literature [26]. Motion control system with DOB is discussed here, therefore trade-off between robustness and performance has been analysed. It has been also shown how DOB is working without outer-loop controller. Frequency responses of inner and outer-loop have been done, for stability analysis root locus plot is also shown. Finally, trajectory tracking has been shown. Chapter 5 is mainly the contribution part. Here, PID controller as outer-loop controller has been used to improve performance than PD controller based DOB. Frequency responses, root locus plots have also been done here. The robustness improvement has been shown by bode plot. Chapter 6 is comparison of performances between existing PD controller based DOB and proposed PID controller based DOB.

7.2 Conclusion:

As stated above, the dissertation verifies the design methods for DOB based motion control system. The trade-off between robustness and performance has also been verified. It is clear from the simulations that velocity estimation plays a great role for robustness, stability and performance. It can be said from comparison report that disturbance estimation is better in case of proposed PID controller and DOB with or without outer-loop controller. In presence of parameter uncertainties the proposed one shows better result. Tracking error is almost same for maximum cases, though in some cases existing method shows better result and vice versa. The analytical derivations are verified by simulations.

7.3 Future scope of work:

In the course of the thesis work, different ideas for future work in this domain emerged:

- Adaptive DOB and RTOB can be implemented for better performance.
- The existing methodologies work well in low frequency range, if DOB based motion control system can perform well in high frequency range then it will be more widely used in industrial applications, i.e. the research are can be extended to high frequency range.
- New controller can be implemented to improve performance.
- Adaptive controllers can be implemented that will give desired response in presence of uncertainties and disturbances.
- Better ways of velocity estimation can be done, that will make the system more robust and stable, hence performance will also be improved.

References

[1]	T. Umeno, T. Kaneko, and Y. Hori, “Robust servosystem design with two degrees of freedom and its application to novel motion control of robot manipulators,” *IEEE Trans. Ind. Electron.*, vol. 40, no. 5, pp. 473–485, Oct. 1993.
[2]	T. Murakami, F. Yu, and K. Ohnishi, “Torque sensorless control in multidegree- of-freedom manipulator,” *IEEE Trans. Ind. Electron.*, vol. 40, no. 2, pp. 259–265, Apr. 1993.
[3]	K. Ohnishi, M. Shibata, and T. Murakami, “Motion control for advanced mechatronics,” *IEEE/ASME Trans.Mechatronics*, vol. 1, no. 1, pp. 56–67, Mar. 1996.
[4]	L. Yi and M. Tomizuka, “Two-degree-of-freedom control with robust feedback control for hard disk servo systems,” *IEEE/ASME Trans.Mechatronics*, vol. 4, no. 1, pp. 17–24, Mar. 1999.
[5]	Z. J. Yang, Y. Fukushima, and P. Qin, “Decentralized adaptive robust control of robot manipulators using disturbance observers,” *IEEE Trans. Control Syst. Technol.*, vol. 20, no. 5, pp. 1357–1365, Sep. 2012.
[6]	A. Suzuki and K. Ohnishi, “Novel four-channel bilateral control design for haptic communication under time delay based on modal space analysis,” *IEEE Trans. Control Syst. Technol.*, vol. 21, no. 3, pp. 882–890, May 2013.
[7]	B. A. Guvenc, L. Guvenc, and S. Karaman, “Robust MIMO disturbance observer analysis and design with application to active car steering,” *Int. J. Robust Nonlinear Control*, vol. 20, no. 8, pp. 873–891, May 2010.
[8]	S. Shimmyo, T. Sato, and K. Ohnishi, “Biped walking pattern generation by using preview control based on three-mass model,” *IEEE Trans. Ind. Electron.*, vol. 60, no. 11, pp. 5137–5147, Nov. 2013.
[9]	C. H. Wai and N. C. Cheung, “Disturbance and response time improvement of submicrometer precision linear motion system by using modified disturbance compensator and internal model reference control,” *IEEE Trans. Ind. Electron.*, vol. 60, no. 1, pp. 139–150, Jan. 2013.
[10]	K. Zhou and Z. Ren, “A new controller architecture for high performance, robust, fault-tolerant control,” *IEEE Trans. Autom. Control*, vol. 46, no. 10, pp. 1613–1618, Oct. 2001.
[11]	S. Katsura, Y. Matsumoto, and K. Ohnishi, “Realization of “Law of action and reaction” by multilateral control,” *IEEE Trans. Ind. Electron.*, vol. 52, no. 5, pp. 1196–1205, Oct. 2005.
[12]	H. Shim and N. H. Jo, “An almost necessary and sufficient condition for robust stability of closed-loop systems with disturbance observer,” *Automatica*, vol. 45, no. 1, pp. 296–299, Jan. 2009.
[13]	A. Šabanovic, “Variable structure systems with sliding modes in motion control—A survey,” *IEEE Trans. Ind. Informat.*, vol. 7, no. 2, pp. 212– 223, May 2011.
[14]	E. Sariyildiz and K. Ohnishi, “Bandwidth constraints of disturbance observer in the presence of real parametric uncertainties,” *Eur. J. Control*, vol. 19, no. 3, pp. 199–205, May 2013.
[15]	E. Sariyildiz and K. Ohnishi, “A guide to design disturbance observer,” *Trans. ASME, J. Dyn. Syst. Meas. Control*, vol. 136, no. 2, pp. 021011-1– 021011-10, Dec. 2014.

[16]	S. Jeon and M. Tomizuka, “Benefits of acceleration measurement in velocity estimation and motion control,” *Control Eng. Pract.*, vol. 15, no. 3, pp. 325–332, Mar. 2007.
[17]	S. Katsura, K. Irie, and K. Ohishi, “Wideband force control by position acceleration integrated disturbance observer,” *IEEE Trans. Ind. Electron.*, vol. 55, no. 4, pp. 1699–1706, Apr. 2008.
[18]	T. T. Phuong, K. Ohishi, Y. Yokokura, and C. Mitsantisuk, “FPGA-based high-performance force control system with friction-free and noise-free force observation,” *IEEE Trans. Ind. Electron.*, vol. 61, no. 2, pp. 994– 1008, Feb. 2014.
[19]	H. Kobayashi, S. Katsura, and K. Ohnishi, “An analysis of parameter variations of disturbance observer for motion control,” *IEEE Trans. Ind. Electron.*, vol. 54, no. 6, pp. 3413–3421, Dec. 2007.
[20]	S. Katsura, Y. Matsumoto, and K. Ohnishi, “Analysis and experimental validation of force bandwidth for force control,” *IEEE Trans. Ind. Electron.*, vol. 53, no. 3, pp. 922–928, Jun. 2006.
[21]	S. Katsura, Y. Matsumoto, and K. Ohnishi, “Modelling of force sensing and validation of disturbance observer for force control,” *IEEE Trans. Ind. Electron.*, vol. 54, no. 1, pp. 530–538, Feb. 2007.
[22]	Y. Ohba *et al.*, “Sensorless force control for injection molding machine using reaction torque observer considering torsion phenomenon,” *IEEE Trans. Ind. Electron.*, vol. 56, no. 8, pp. 2955–2960, Aug. 2009.
[23]	E. Sariyildiz and K. Ohnishi, “An adaptive reaction force observer design,” *IEEE/ASME Trans. Mechatronics*, vol. 20, no. 2, pp. 750–760, Apr. 2015.
[24]	E. Sariyildiz and K. Ohnishi, “ Stability and robustness of disturbance observer based motion control system”, IEEE *Transaction on Industrial Electronics*, vol. 62, NO. 1, Jan. 2015
[25]	https://en.wikipedia.org/wiki/Motion_control
[26]	S. Li, J. Yang, W.H. Chen, X. Chen, *Disturbance Observer Based control-Methods and Applications*.
[27]	P. Cominos, N. Munro, “PID controllers: recent tuning methods and design to specification,” *IEE Proc.-Control Theory Appl.*, vol. 149, no. 1, pp. 46-53, Jan., 2002.
[28]	J. Han, P. Wang, X. Yang, “Tuning of PID controller based on fruit fly optimization algorithm,” in *Internaional Conference on Mechatronics and Automation (ICMA)*, 2012, pp. 409-413.
[29]	W. K. Ho, 0. P. Gan, E. B. Tay, E. L. Ang, “Performance and Gain and Phase Margins of Well-Known PID Tuning Formulas,” *IEEE Transactions on Control Systems Technology*, vol. 4, no. 4, pp. 473-477, July, 1996.
[30]	O.Ozen, E. Sariyildiz, H.Yu, K.Ogawa, K. Ohnishi, A. Sabanovic, “ Practical PID Controller Tuning for Motion Control”, in *IEEE International Conference on Mechatronics (ICM)*, pp.240-245, March, 2015